

Silicon-Germanium Ring Resonator On-Chip with High Q-factor in the Mid-Infrared

Marko Perestjuk^{1,2}, Rémi Armand², Alberto Della Torre², Milan Sinobad³, Arnan Mitchell¹, Andreas Boes^{1,4}, Jean-Michel Hartmann⁵, Jean-Marc Fedeli⁵, Vincent Reboud⁵, Alfredo de Rossi⁶, Sylvain Cmbrié⁶, Christelle Monat² and Christian Grillet²

¹Integrated Photonics and Applications Centre, School of Engineering, RMIT University, Melbourne, VIC 3001, Australia

²Université de Lyon, Institut des Nanotechnologies de Lyon (INL, UMR-CNRS 5270), Ecole Centrale de Lyon, 69130 Ecully, France

³Deutsches Elektronen-Synchrotron, 22607 Hamburg, Germany

⁴Institute for Photonics and Advanced Sensing, The University of Adelaide, Adelaide, SA 5005, Australia

⁵CEA-Leti, Université Grenoble Alpes, 38054 Grenoble Cedex 9, France

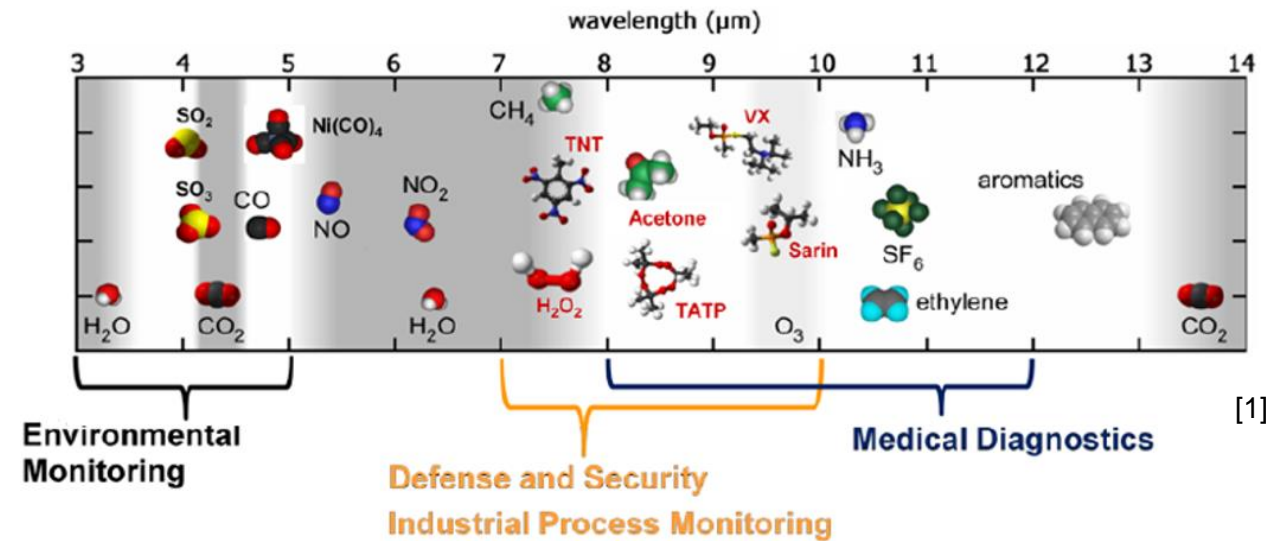
⁶Thales Research and Technology, Campus Polytechnique, Palaiseau, France



“Silicon-Germanium Ring Resonator On-Chip with High Q-factor in the Mid-Infrared”

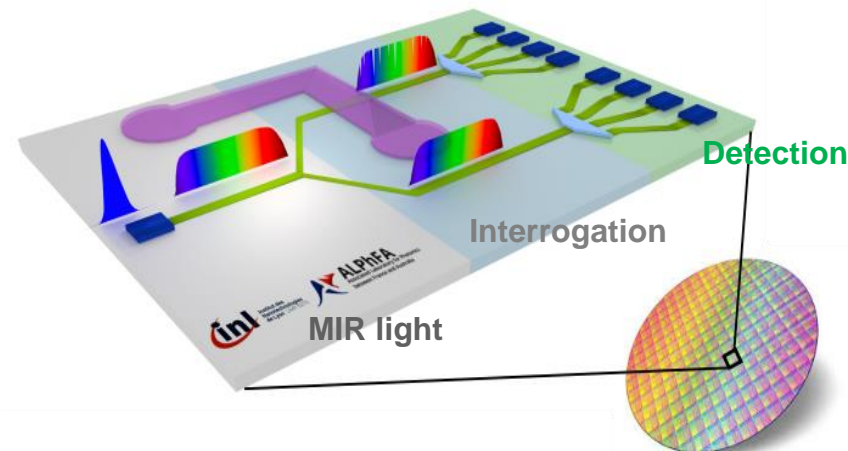
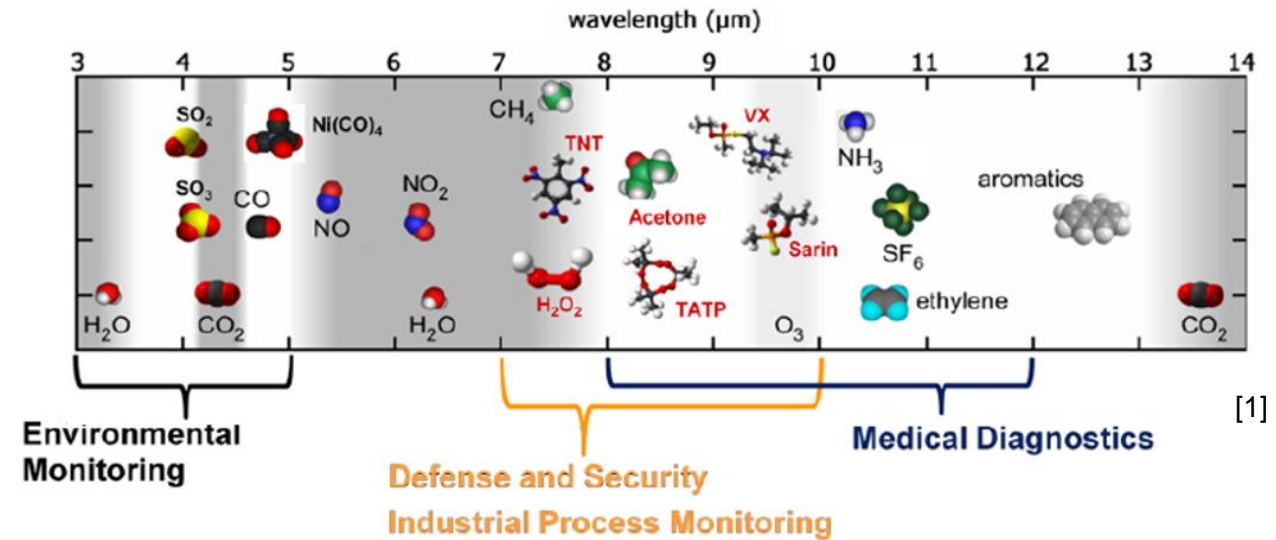
- Introduction
 - Why Mid-Infrared?
 - Why Silicon Germanium?
 - Why High Q ring resonators?
 - State of the art
- Design and fabrication of ring
- Loss and Q-factor measurement
- Simulation of frequency comb generation

- Fundamental absorption lines of many molecules in the MIR
 → high application potential



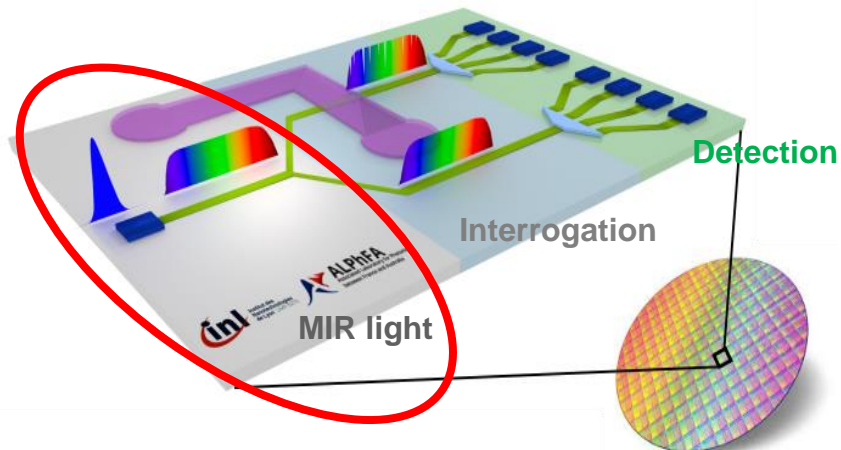
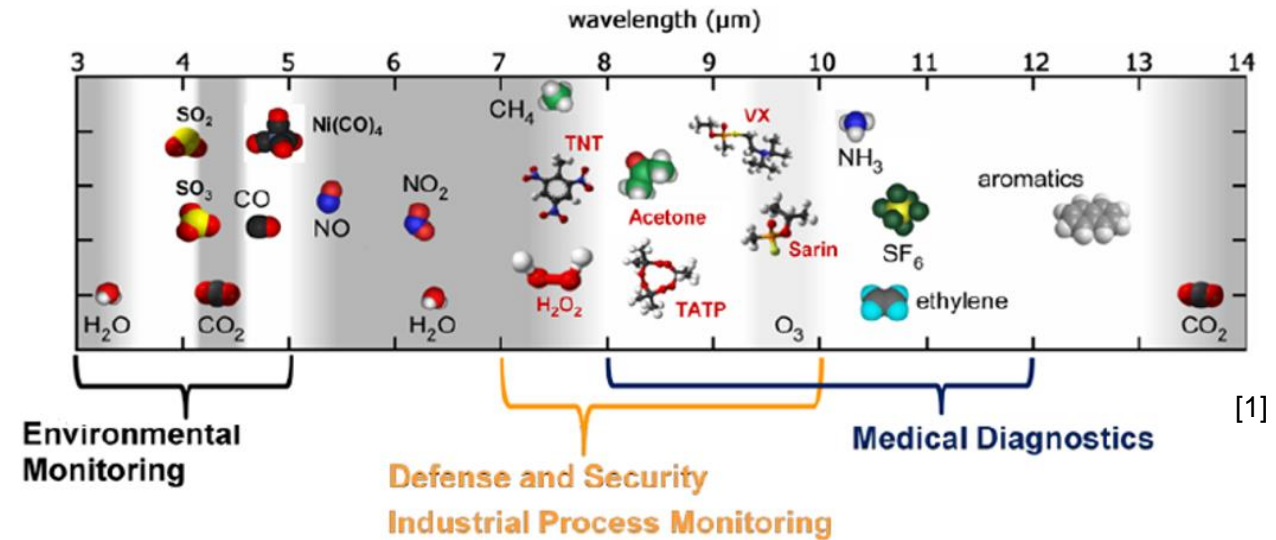
[1] D. Caffey et al., Photonics West 2011

- Fundamental absorption lines of many molecules in the MIR
 - high application potential
- Lack of compact and low cost devices
- Proposed MIR sensor system



[1] D. Caffey et al., Photonics West 2011

- Fundamental absorption lines of many molecules in the MIR
 - high application potential
- Lack of compact and low cost devices
- Proposed MIR sensor system



[1] D. Caffey et al., Photonics West 2011

Through Nonlinear Optics

$$\text{Wave equation : } \nabla \times \nabla \times E(r, t) + \frac{1}{c^2} \frac{\partial^2 E(r, t)}{\partial t^2} = -\mu_0 \frac{\partial^2 P(r, t)}{\partial t^2}$$

$$P = \varepsilon_0 (\chi^{(1)} \cdot E) + \varepsilon_0 (\chi^{(2)} \cdot EE + \chi^{(3)} \cdot EEE + \dots)$$

Through Nonlinear Optics

$$\text{Wave equation : } \nabla \times \nabla \times E(r, t) + \frac{1}{c^2} \frac{\partial^2 E(r, t)}{\partial t^2} = -\mu_0 \frac{\partial^2 P(r, t)}{\partial t^2}$$

$$P = \underbrace{\varepsilon_0 (\chi^{(1)} \cdot E)}_{\text{linear}} + \underbrace{\varepsilon_0 (\chi^{(2)} \cdot EE + \chi^{(3)} \cdot EEE + \dots)}_{\text{nonlinear}}$$

- Absorption
- Dispersion



linear

nonlinear



- Four wave mixing
- Self phase modulation
- Cross phase modulation
- Soliton fission
- Raman scattering
- Brillouin scattering
- ...

Through Nonlinear Optics

$$\text{Wave equation : } \nabla \times \nabla \times E(r, t) + \frac{1}{c^2} \frac{\partial^2 E(r, t)}{\partial t^2} = -\mu_0 \frac{\partial^2 P(r, t)}{\partial t^2}$$

$$P = \underbrace{\varepsilon_0 (\chi^{(1)} \cdot E)}_{\text{linear}} + \underbrace{\varepsilon_0 (\cancel{\chi^{(2)} EE} + \chi^{(3)} \cdot EEE + \dots)}_{\text{nonlinear}}$$

- Absorption
- Dispersion



linear

nonlinear



- Four wave mixing
- Self phase modulation
- Cross phase modulation
- Soliton fission
- Raman scattering
- Brillouin scattering
- ...

Through Nonlinear Optics

$$\text{Wave equation : } \nabla \times \nabla \times E(r, t) + \frac{1}{c^2} \frac{\partial^2 E(r, t)}{\partial t^2} = -\mu_0 \frac{\partial^2 P(r, t)}{\partial t^2}$$

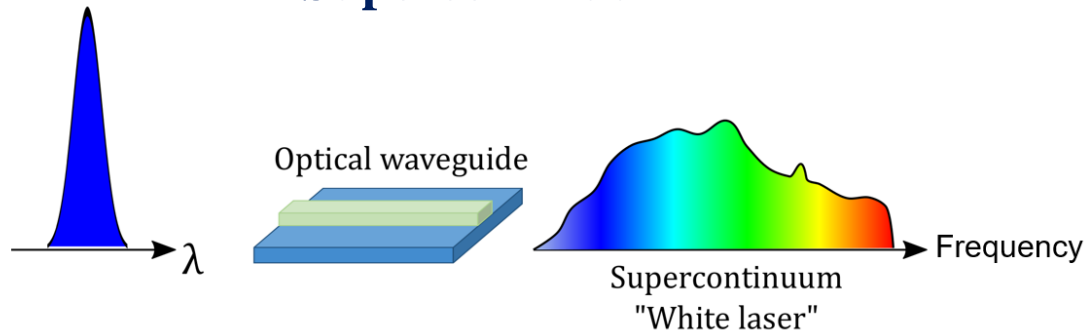
$$P = \underbrace{\varepsilon_0 (\chi^{(1)} \cdot E)}_{\text{linear}} + \underbrace{\varepsilon_0 (\cancel{\chi^{(2)} \cdot EE} + \chi^{(3)} \cdot EEE + \dots)}_{\text{nonlinear}}$$

- Absorption
- Dispersion

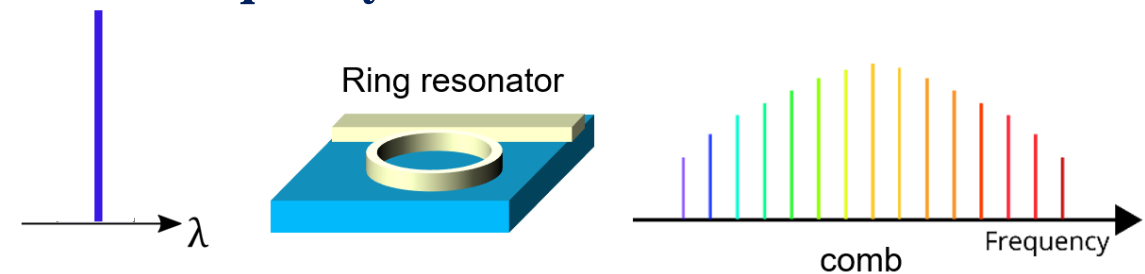
- Four wave mixing
- Self phase modulation
- Cross phase modulation
- Soliton fission
- Raman scattering
- Brillouin scattering
- ...

Two options for broadband sources:

Supercontinuum



Frequency Comb



Through Nonlinear Optics

$$\text{Wave equation : } \nabla \times \nabla \times E(r, t) + \frac{1}{c^2} \frac{\partial^2 E(r, t)}{\partial t^2} = -\mu_0 \frac{\partial^2 P(r, t)}{\partial t^2}$$

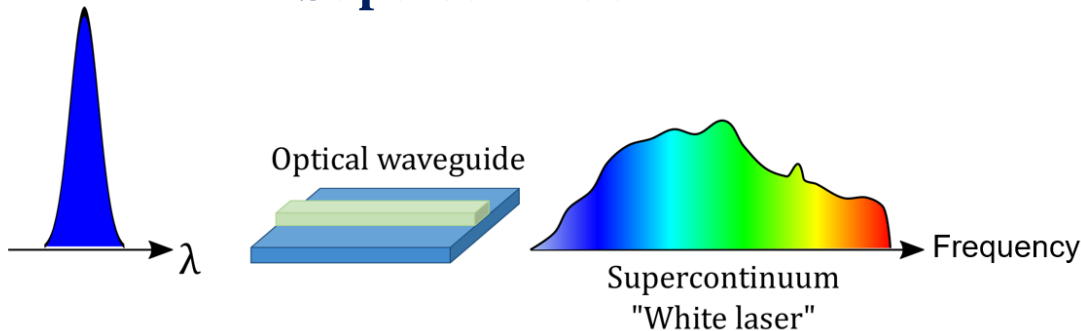
$$P = \underbrace{\varepsilon_0 (\chi^{(1)} \cdot E)}_{\text{linear}} + \underbrace{\varepsilon_0 (\cancel{\chi^{(2)} \cdot EE} + \chi^{(3)} \cdot EEE + \dots)}_{\text{nonlinear}}$$

- Absorption
- Dispersion

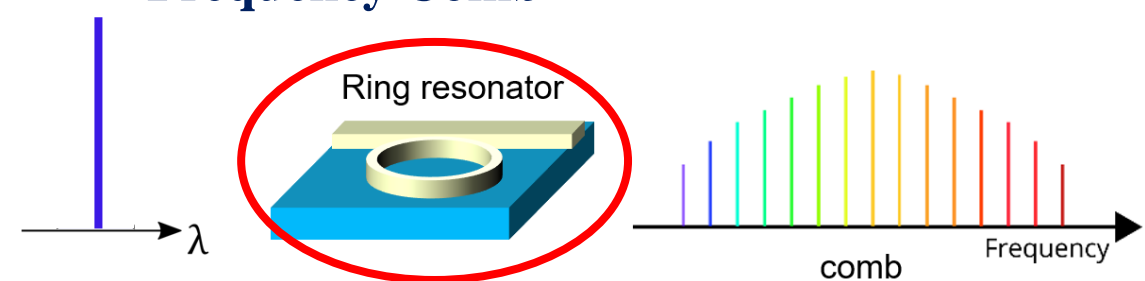
- Four wave mixing
- Self phase modulation
- Cross phase modulation
- Soliton fission
- Raman scattering
- Brillouin scattering
- ...

Two options for broadband sources:

Supercontinuum



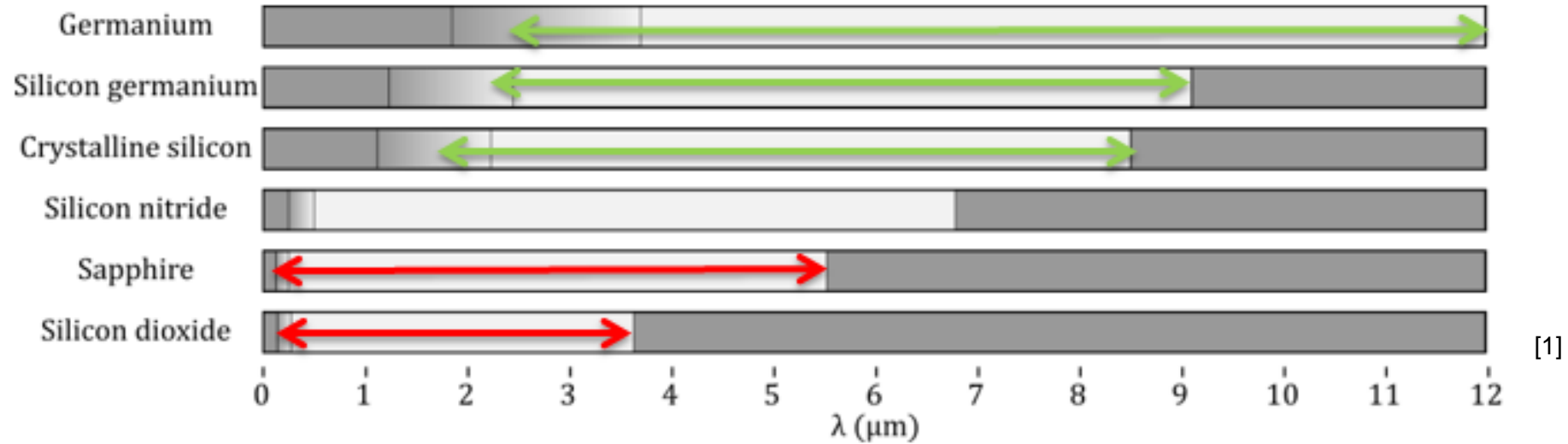
Frequency Comb



Cavities are a crucial building block

But: many linear applications also possible for sensing

Transparency Window of Group IV Materials

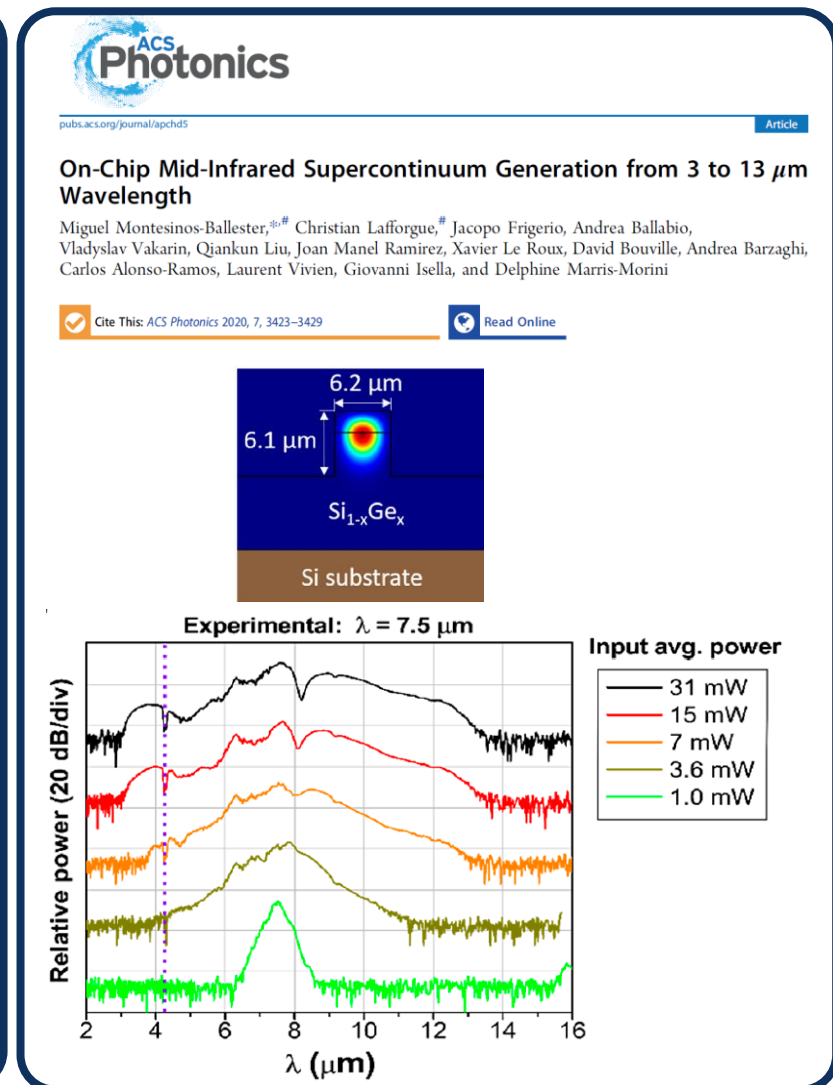
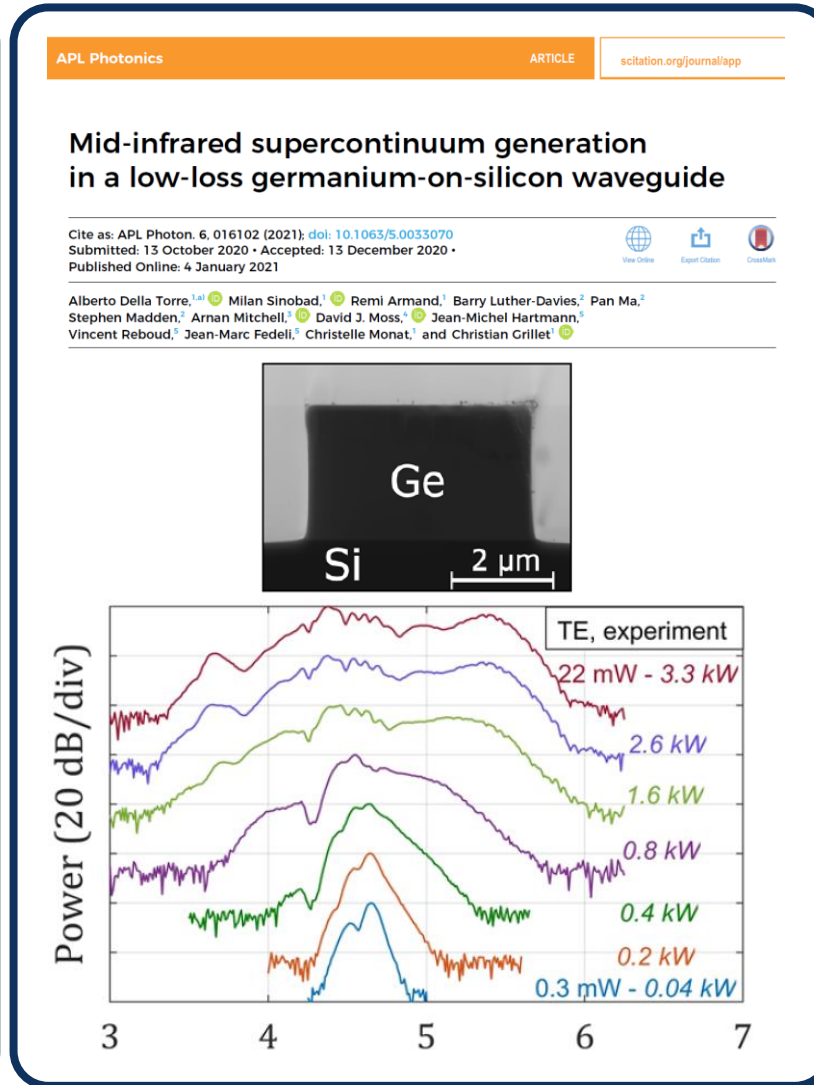
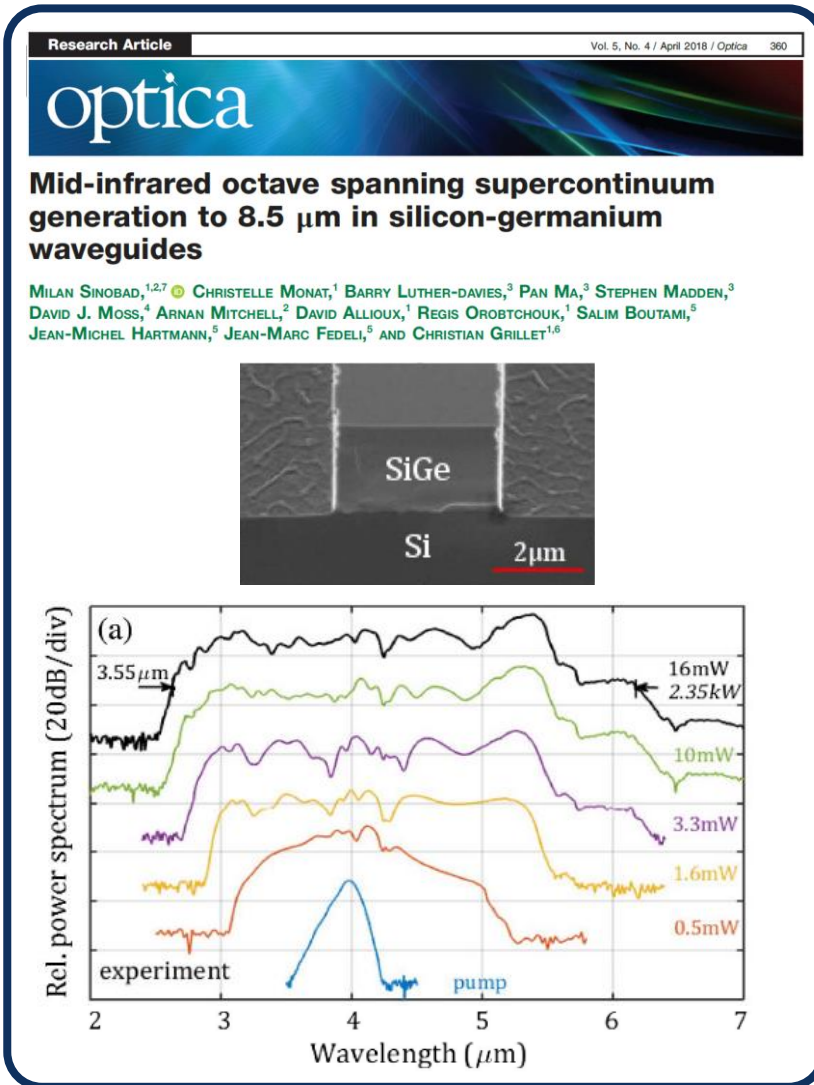


- SOI has strong absorption beyond 3.5μm wavelength due to the silicon dioxide
- SiGe and Ge based waveguides transparent deep into the MIR
- CMOS compatible
- Low loss and nonlinearities demonstrated in SiGe and Ge [2]

[1] adapted from: Soref, Richard, *Mid-infrared photonics in silicon and germanium*, Nature photonics vol. 4, no. 8, pp. 495-497, 2010

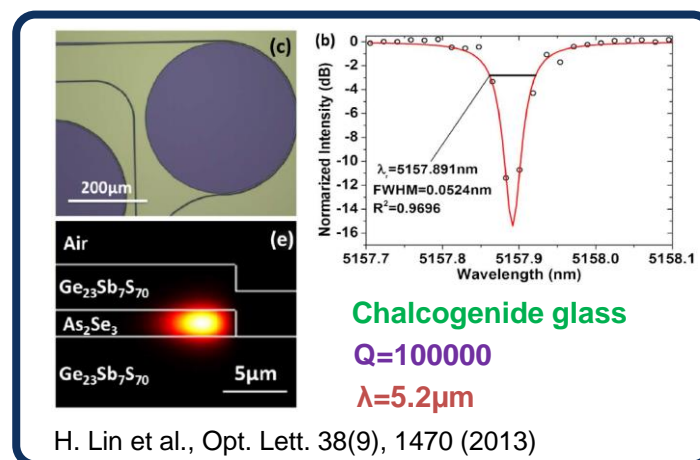
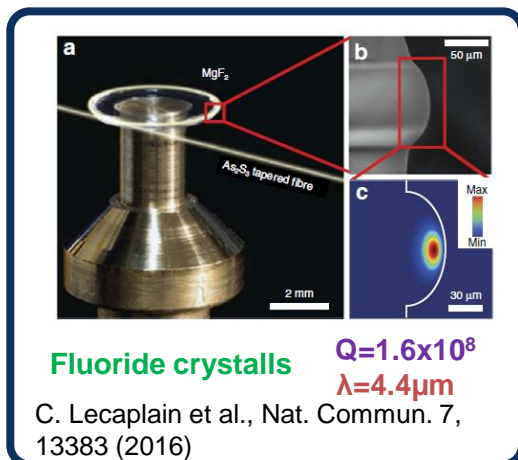
[2] L. Carletti, *et al.*, *Nonlinear optical response of low loss silicon germanium waveguides in the mid-infrared*, Opt Express, vol. 23, no. 7, pp. 8261-8271, 2015

Fast Progress in the Last Years

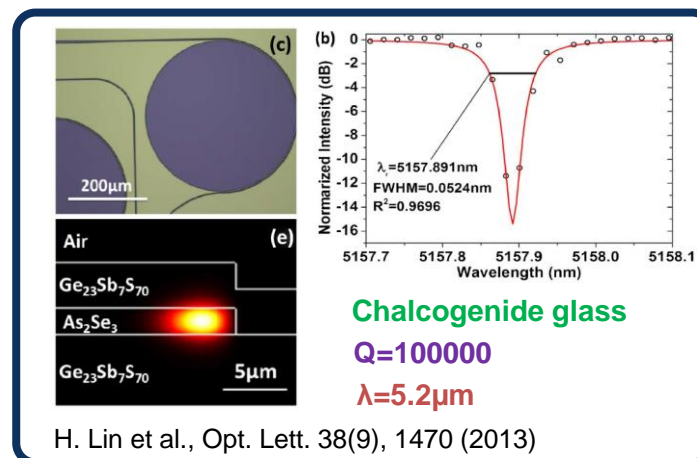
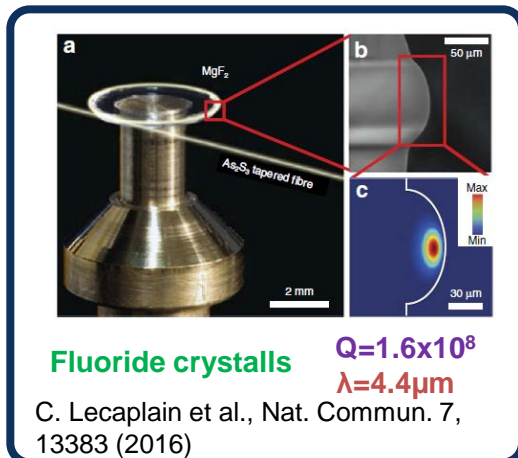
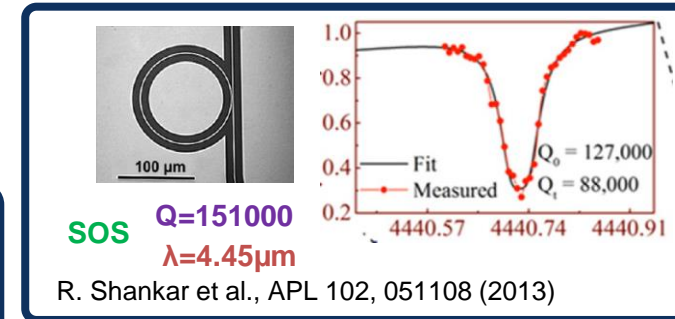
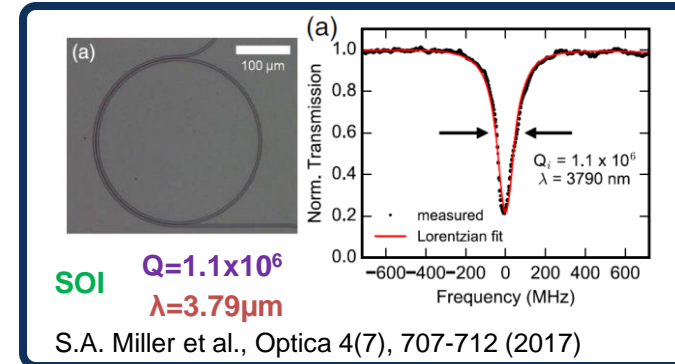


- Impressive results over the past years
- But: Demonstrations of cavities in the MIR so far lack at least one of the following:
 - Integrability
 - CMOS compatibility
 - High Q-factor
 - Sufficiently long λ

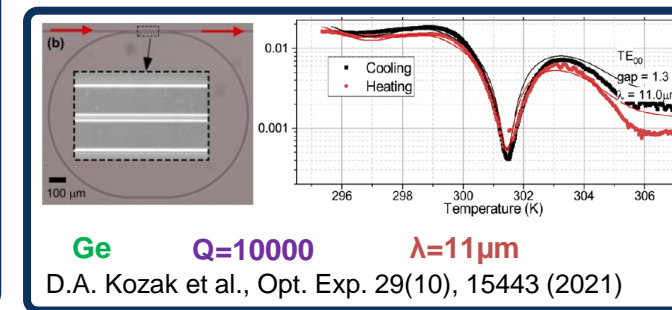
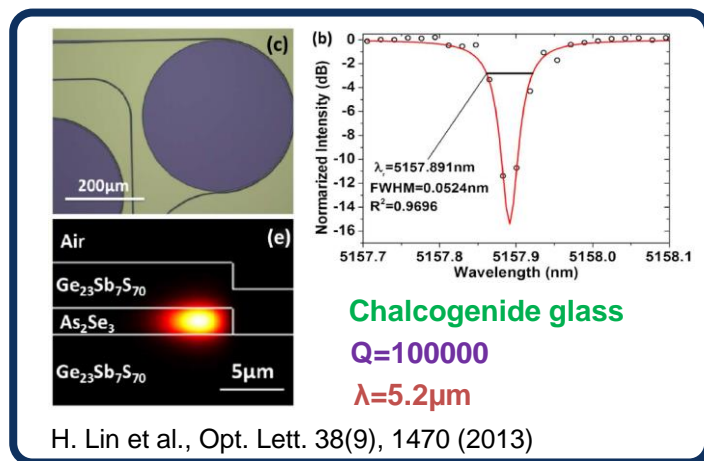
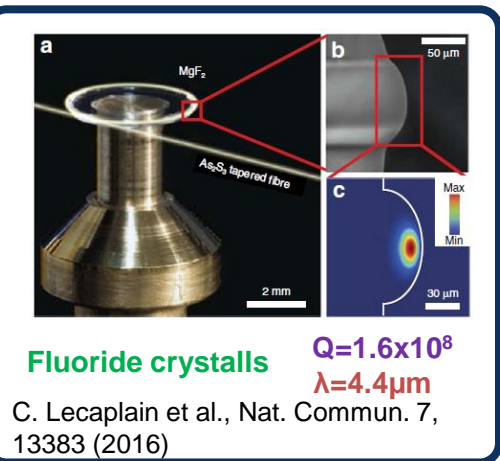
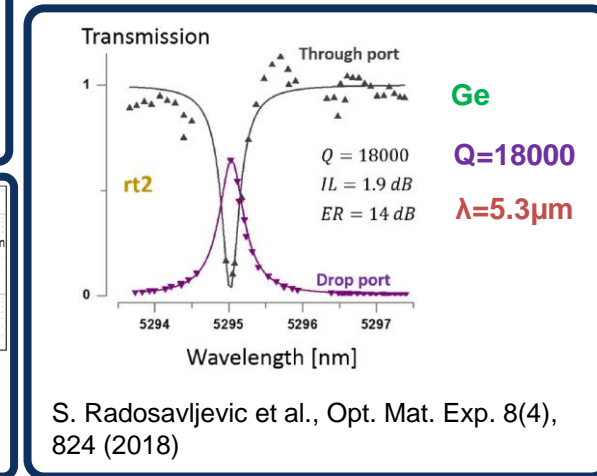
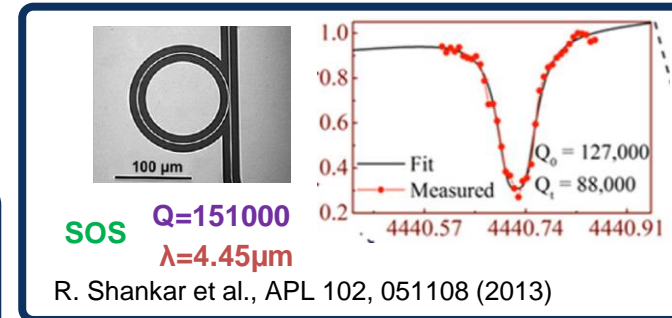
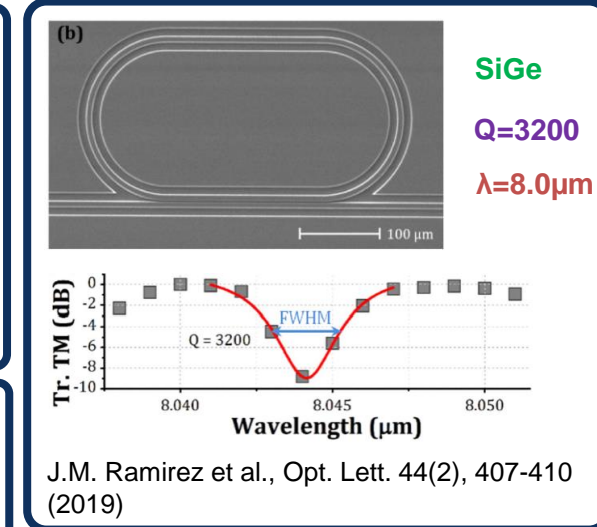
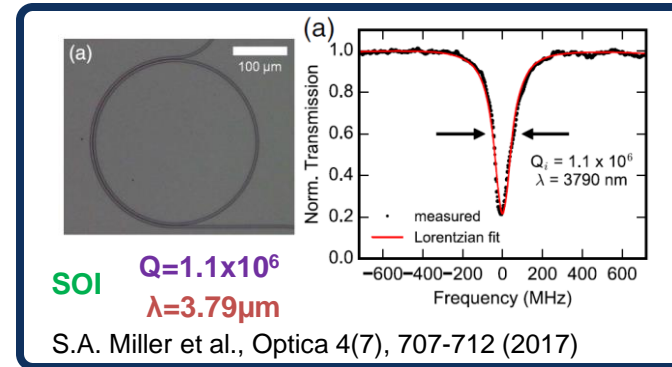
- Impressive results over the past years
- But: Demonstrations of cavities in the MIR so far lack at least one of the following:
 - Integrability
 - CMOS compatibility
 - High Q-factor
 - Sufficiently long λ



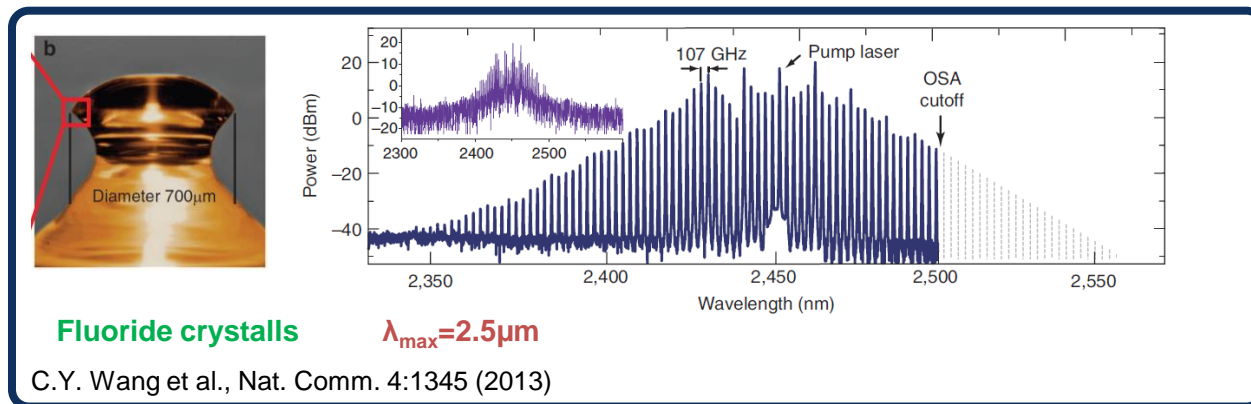
- Impressive results over the past years
- But: Demonstrations of cavities in the MIR so far lack at least one of the following:
 - Integrability
 - CMOS compatibility
 - High Q-factor
 - Sufficiently long λ



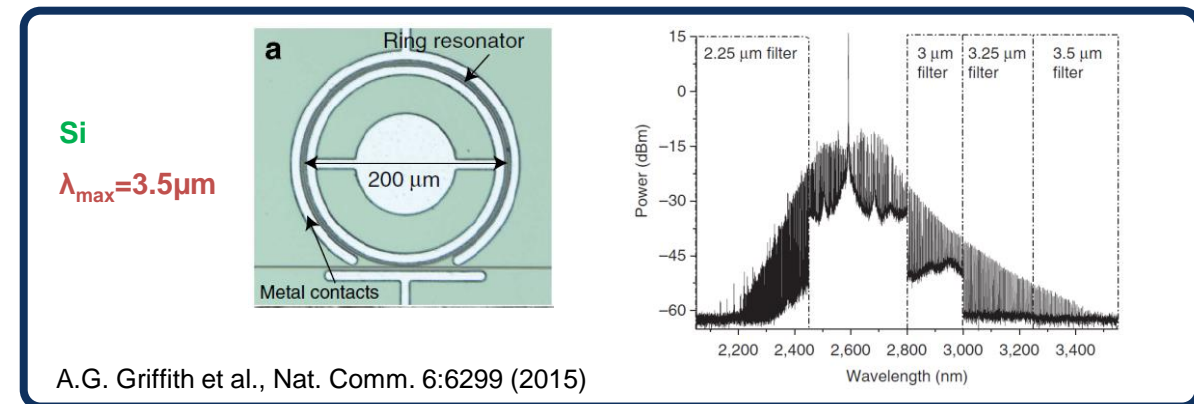
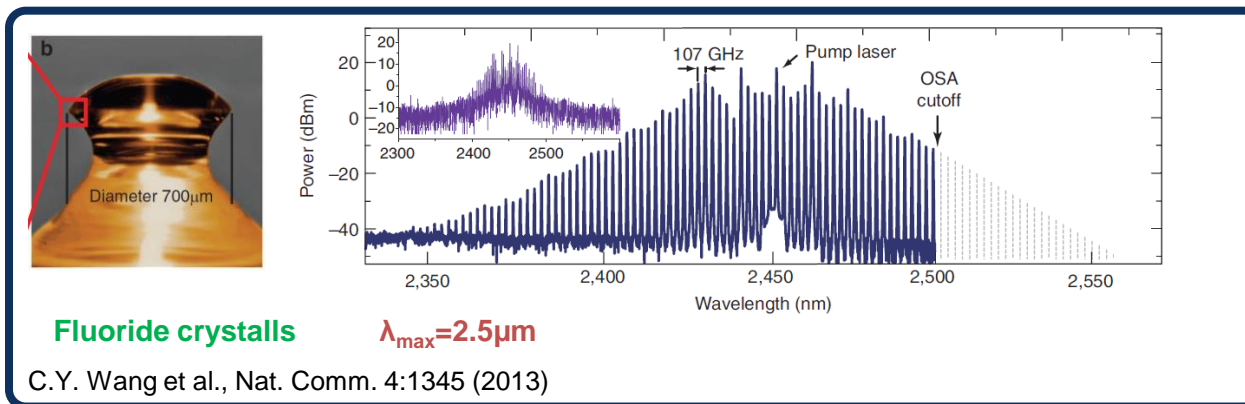
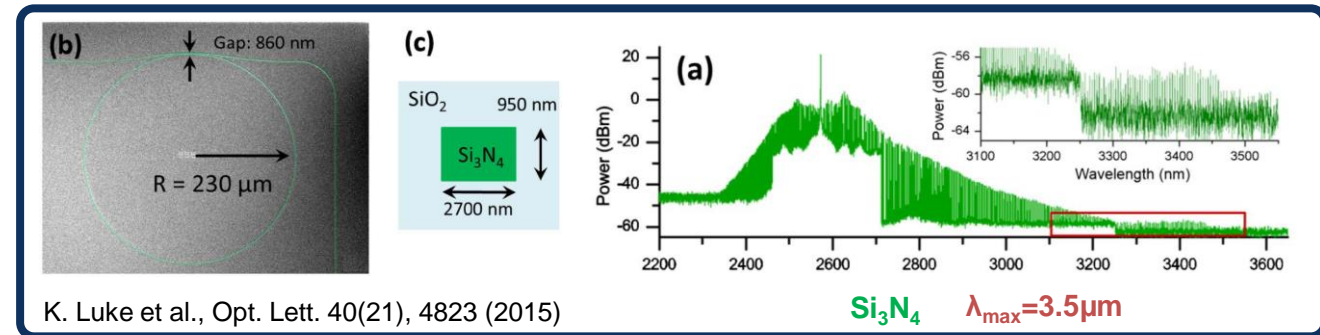
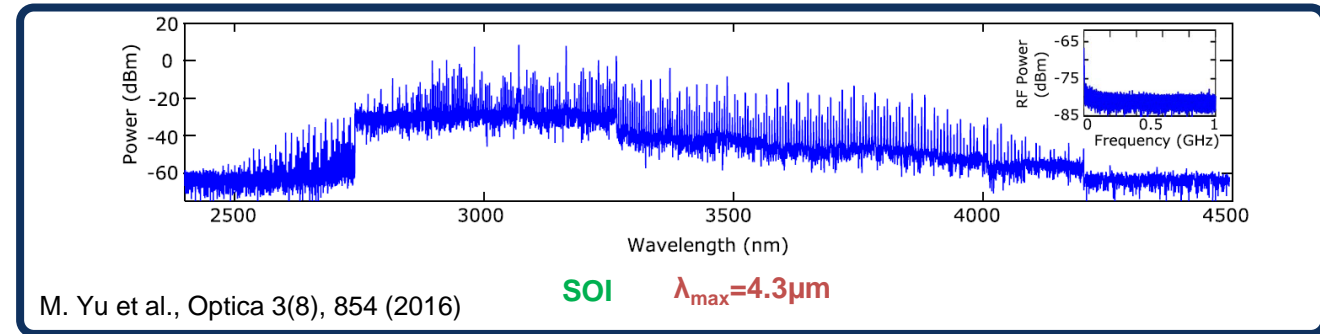
- Impressive results over the past years
- But: Demonstrations of cavities in the MIR so far lack at least one of the following:
 - Integrability
 - CMOS compatibility
 - High Q-factor
 - Sufficiently long λ



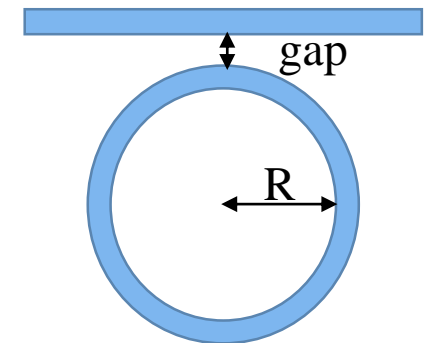
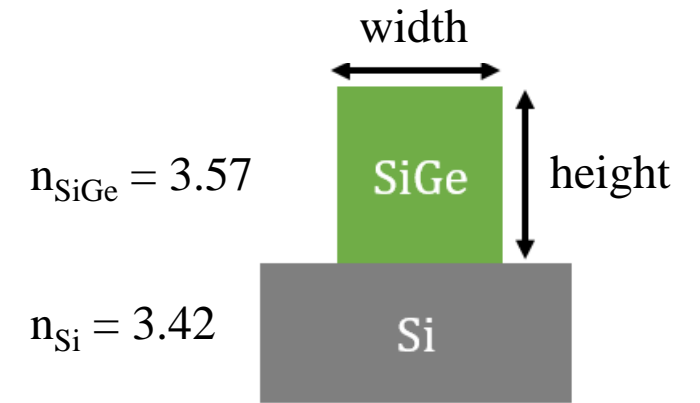
- Again, very impressive results, but:
- Demonstrations of combs in the MIR have the same problems as cavities:
 - No integrability
 - No CMOS compatibility
 - Not sufficiently long λ



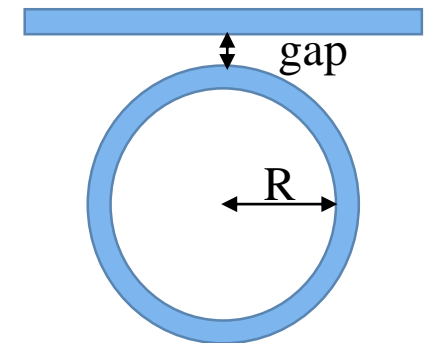
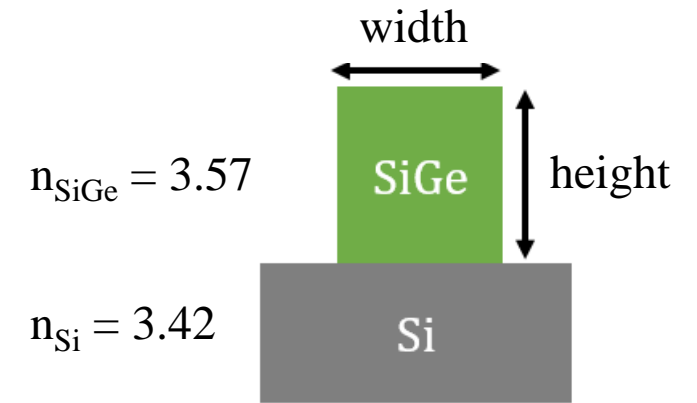
- Again, very impressive results, but:
- Demonstrations of combs in the MIR have the same problems as cavities:
 - No integrability
 - No CMOS compatibility
 - Not sufficiently long λ



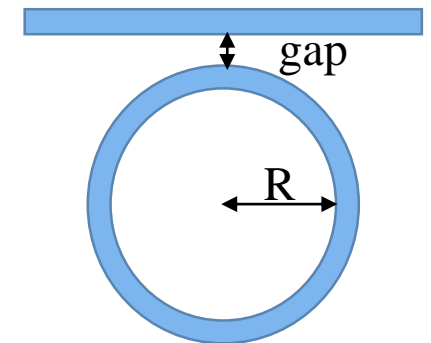
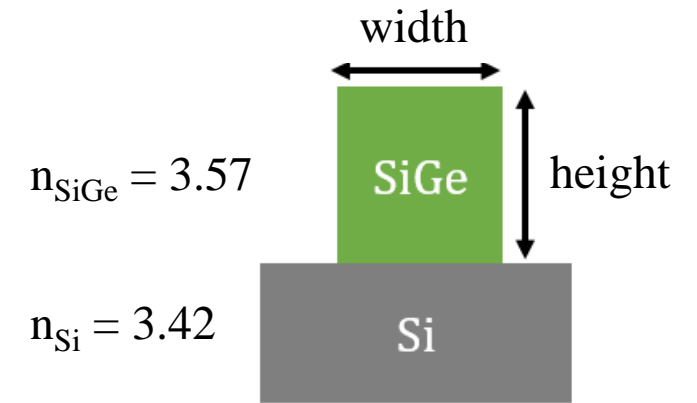
- Suitable for frequency comb generation
 - Anomalous dispersion required
 - This will determine width/height



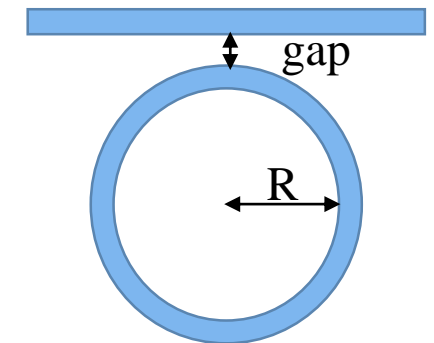
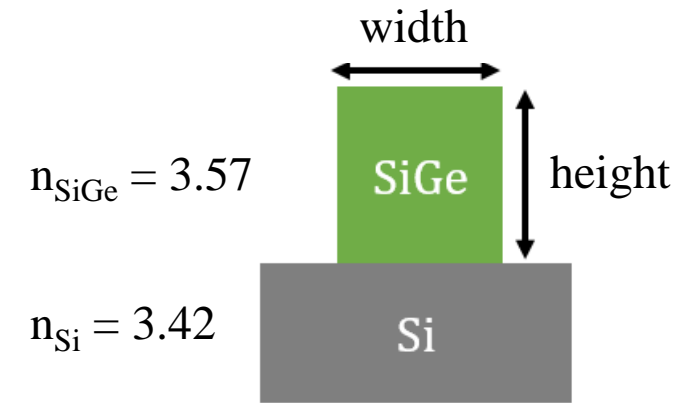
- Suitable for frequency comb generation
 - Anomalous dispersion required
 - This will determine width/height
- Have a free spectral range (FSR) useful for sensing applications
 - $R = 250\mu\text{m}$ (FSR of 53GHz)



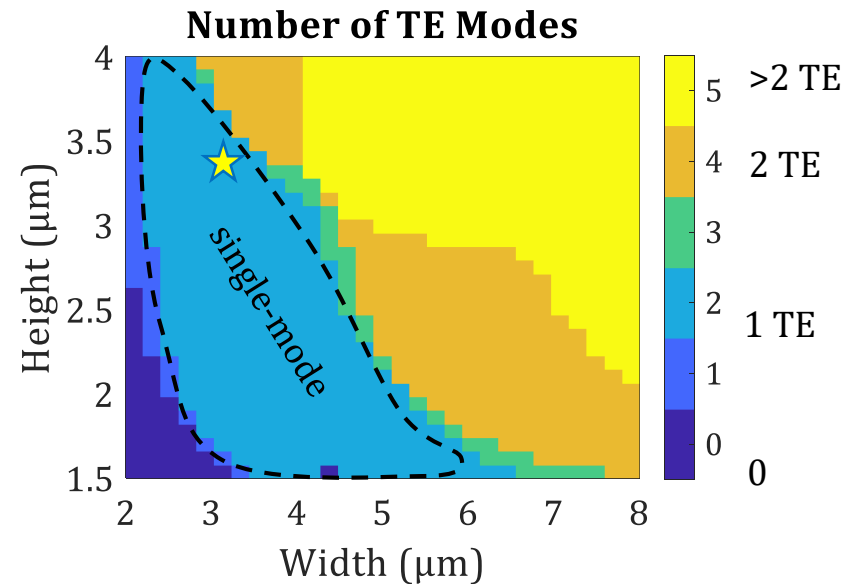
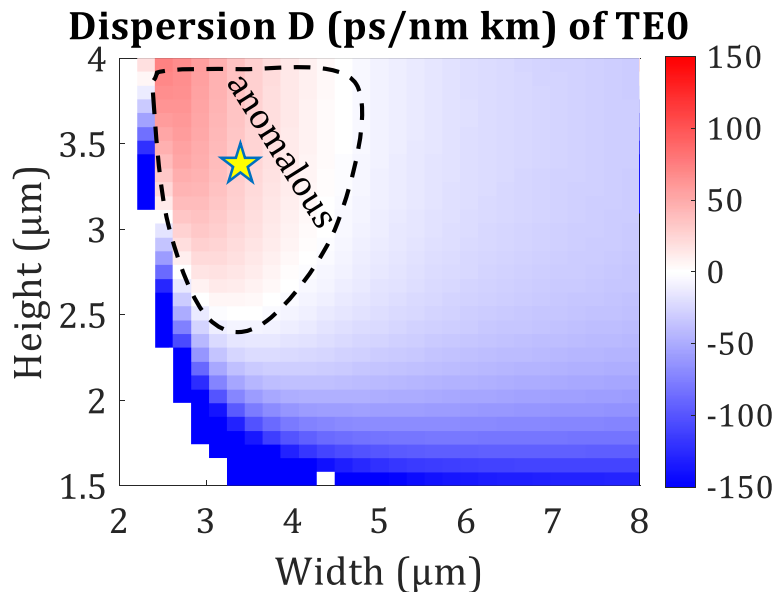
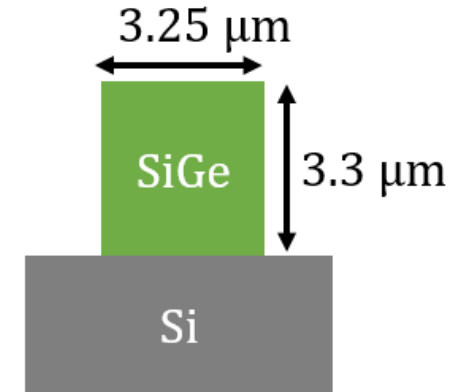
- Suitable for frequency comb generation
 - Anomalous dispersion required
 - This will determine width/height
- Have a free spectral range (FSR) useful for sensing applications
 - $R = 250\mu\text{m}$ (FSR of 53GHz)
- High Q
 - Reduce bending loss, lower bound for $R = 250\mu\text{m}$



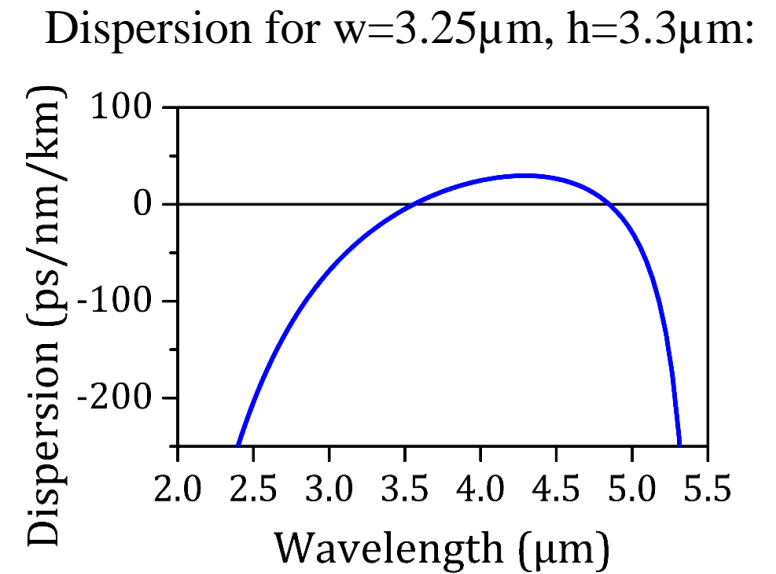
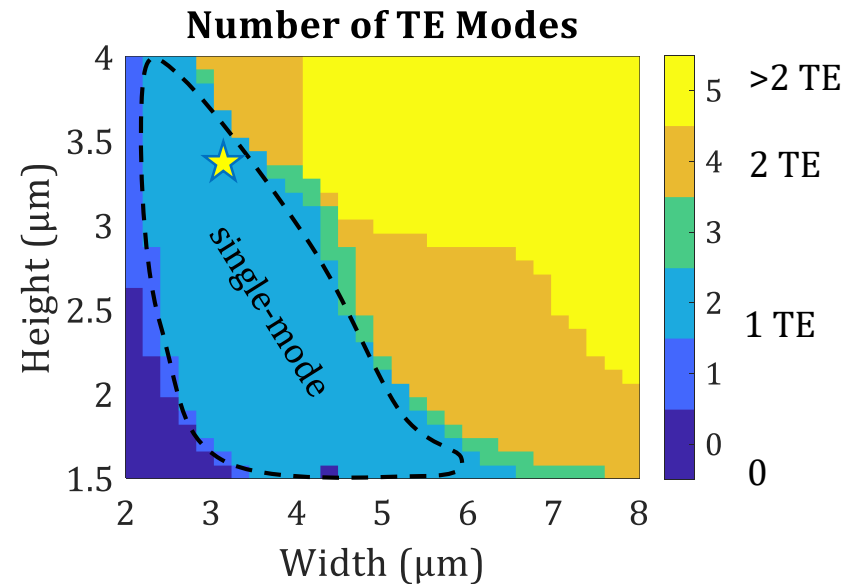
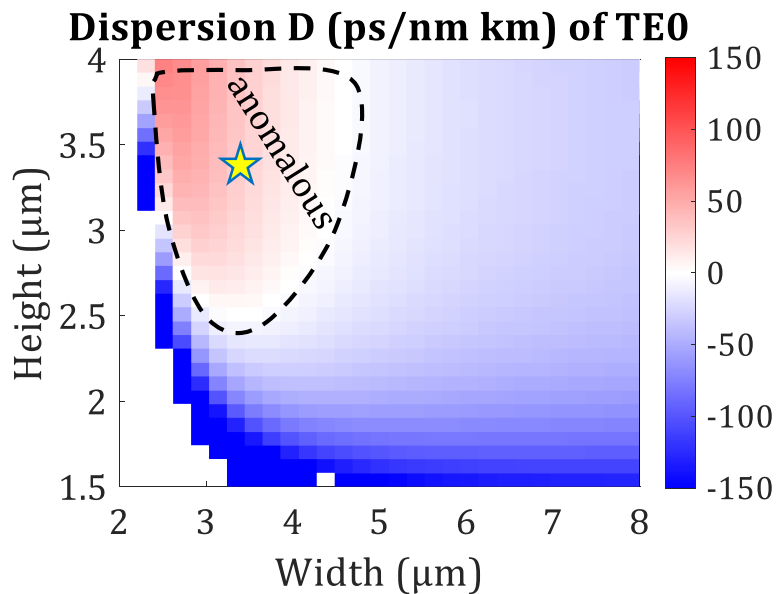
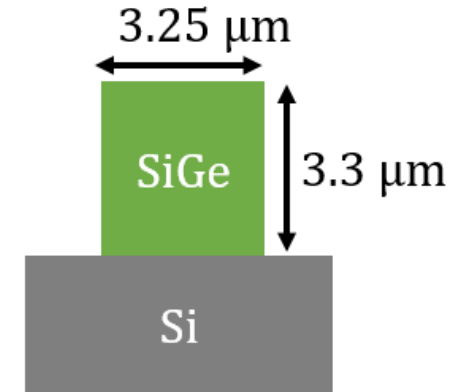
- Suitable for frequency comb generation
 - Anomalous dispersion required
 - This will determine width/height
- Have a free spectral range (FSR) useful for sensing applications
 - $R = 250\mu\text{m}$ (FSR of 53GHz)
- High Q
 - Reduce bending loss, lower bound for $R = 250\mu\text{m}$
- Aiming for critical coupling
 - $\text{gap} = 250\text{nm}$ (smallest achievable gap in fabrication)



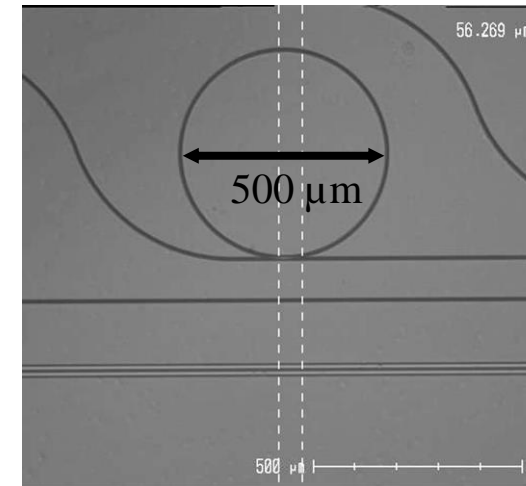
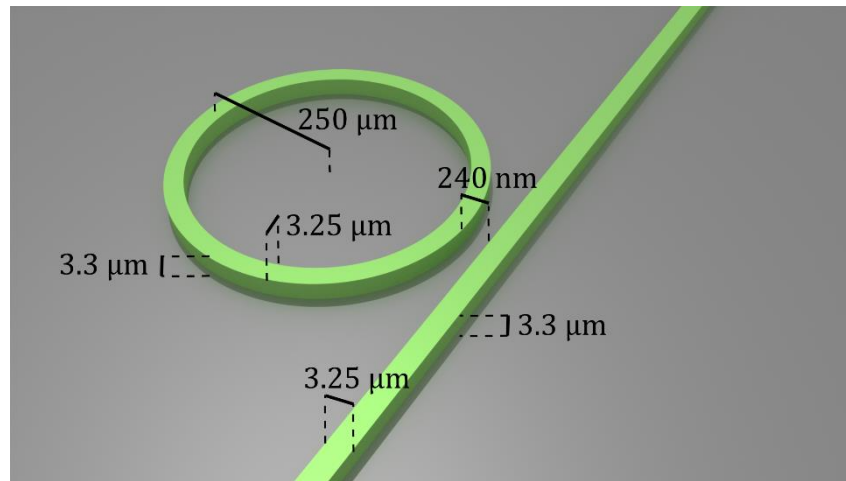
- Operating in TE polarization
- Pump wavelength $\lambda = 4.18\mu\text{m}$
- Single-mode
- Sufficiently large region with anomalous dispersion



- Operating in TE polarization
- Pump wavelength $\lambda = 4.18\mu\text{m}$
- Single-mode
- Sufficiently large region with anomalous dispersion



- $\text{Si}_{0.6}\text{Ge}_{0.4}$ waveguide (air-cladded) on Si substrate
- Deep UV photolithography
- 200mm CMOS pilot line at CEA-Leti

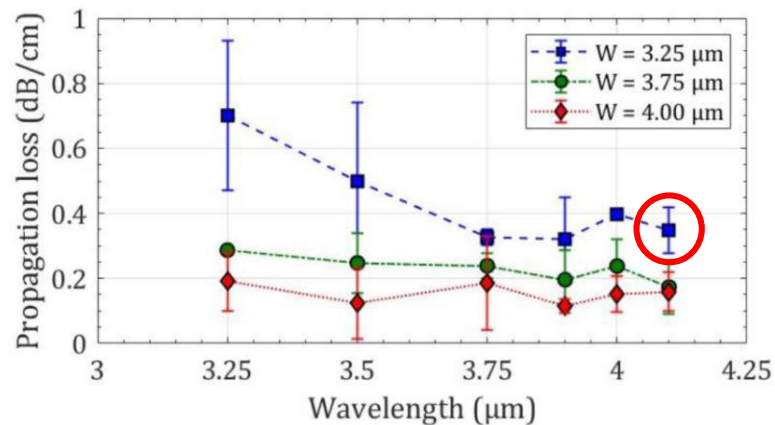


	Radius (μm)	Width (μm)	Gap (nm)
Range of parameters	80, 130, 180, 250	3.25, 3.50, 3.75	250, 500, 750, 1000
Featured value	250	3.25	250



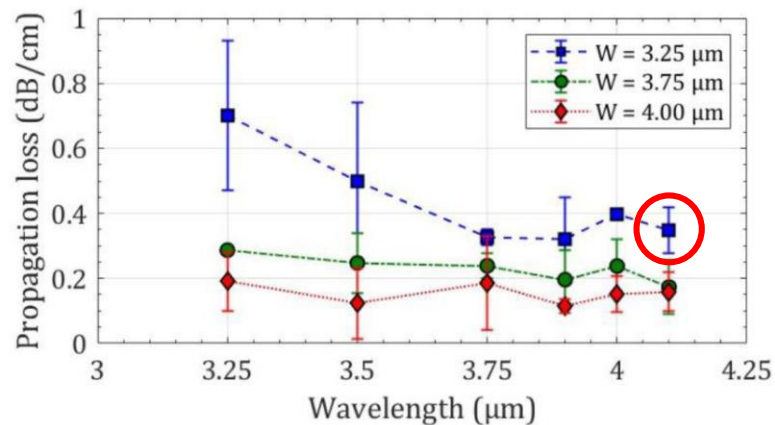
Propagation loss:

- Loss measurement from spirals with different lengths (TE)
- 0.35 dB/cm propagation loss for $w = 3.25\mu\text{m}$
 - Estimated $Q_{\text{int}} = 680,000$
- Even 0.18 dB/cm for $w = 3.75\mu\text{m}$, but difficult to couple



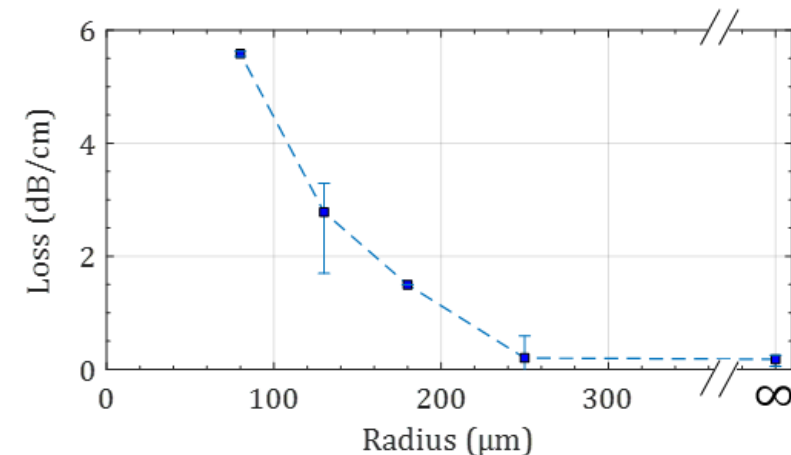
Propagation loss:

- Loss measurement from spirals with different lengths (TE)
- 0.35 dB/cm propagation loss for $w = 3.25\mu\text{m}$
 - Estimated $Q_{\text{int}} = 680,000$
- Even 0.18 dB/cm for $w = 3.75\mu\text{m}$, but difficult to couple



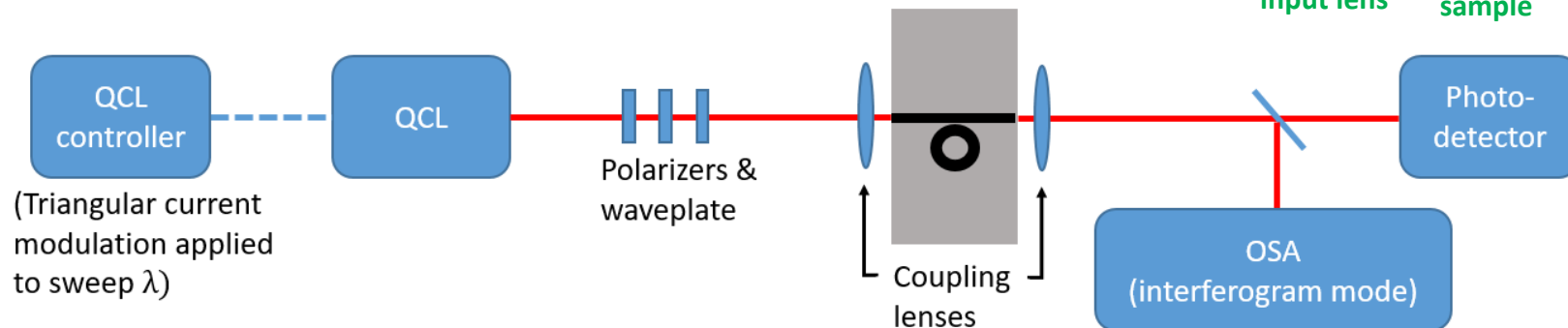
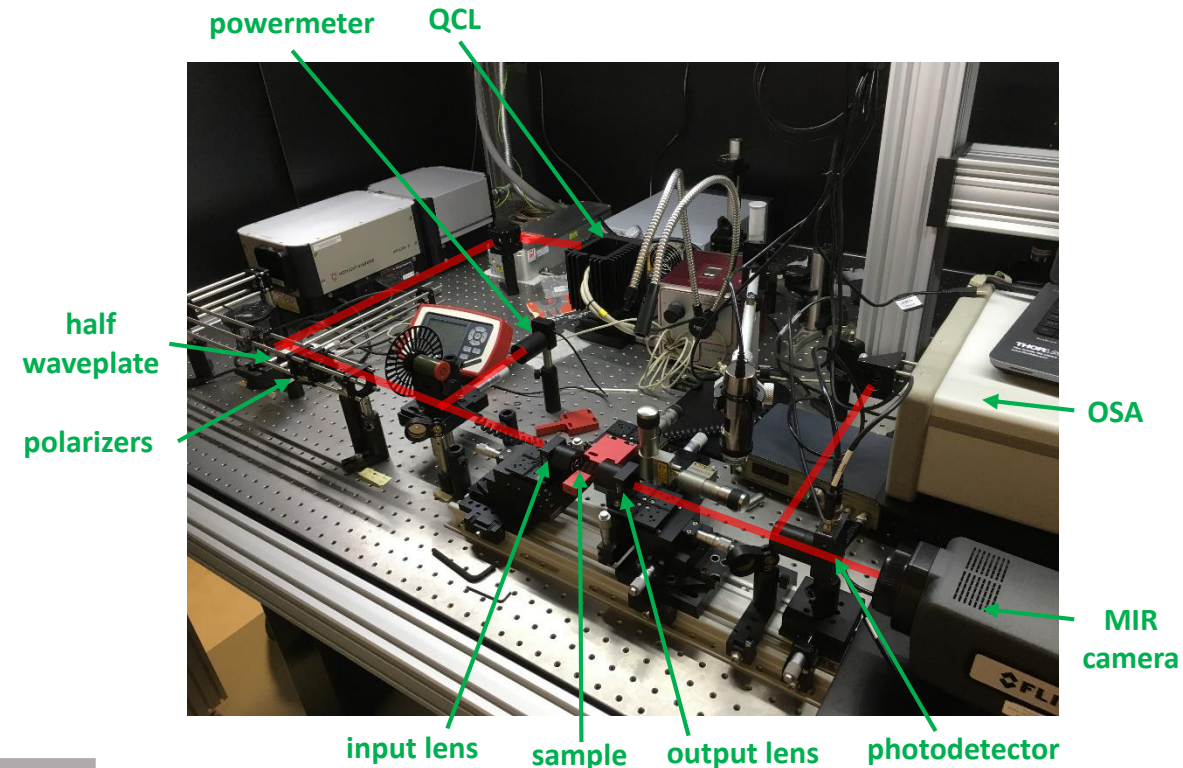
Bending loss:

- Loss measurement from snake waveguides (TE)
- $R=250\mu\text{m}$ shows almost no difference to straight waveguide



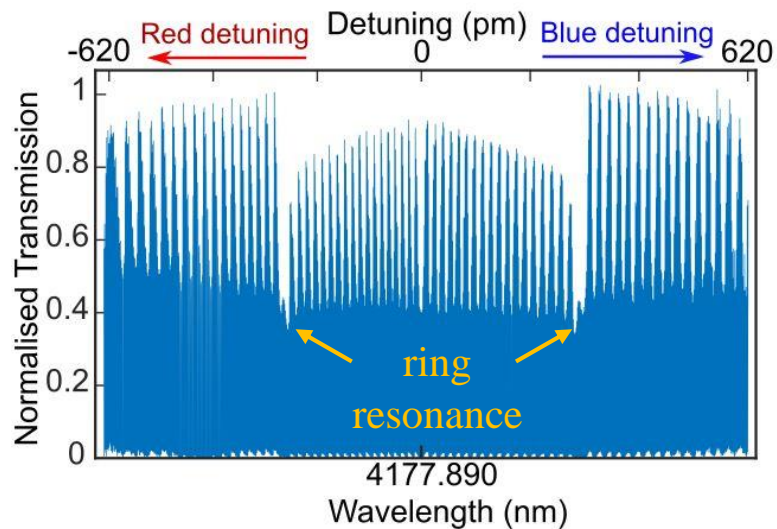
Q-factor characterization

- cw QCL around $4.18\mu\text{m}$
- But-coupling to the chip
- Wavelength sweep (4177.58 ± 0.31) nm (periodic, achieved by triangular current modulation)
- Coupled power: 20 mW (side effect: there is also a power modulation)

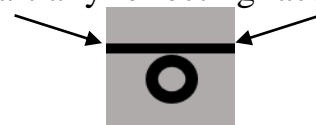


First High-Q Ring on SiGe in the MIR

- Spectrum shows ring resonance and Fabry-Perot resonances from chip facets



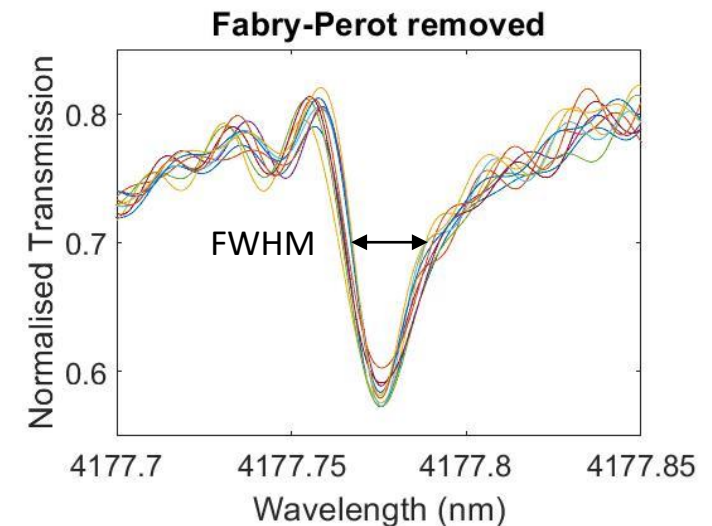
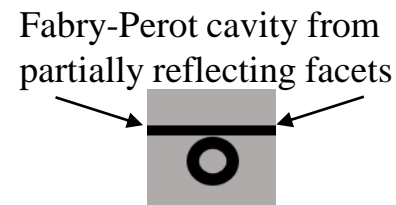
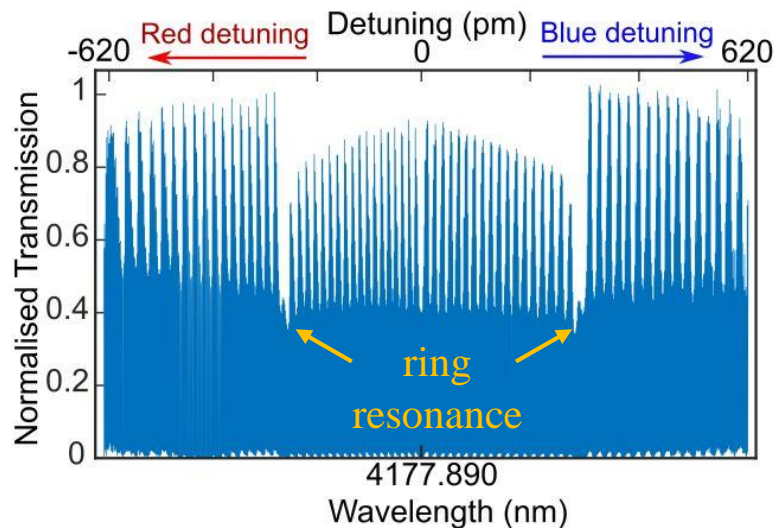
Fabry-Perot cavity from partially reflecting facets



First High-Q Ring on SiGe in the MIR

- Spectrum shows ring resonance and Fabry-Perot resonances from chip facets
- Fourier filtering to remove Fabry-Perot effect
- FWHM = 23pm (corresponds to $Q_{\text{tot}} = 176,000$)

$$\frac{1}{Q_{\text{tot}}} = \frac{1}{Q_{\text{coup}}} + \frac{1}{Q_{\text{int}}}$$

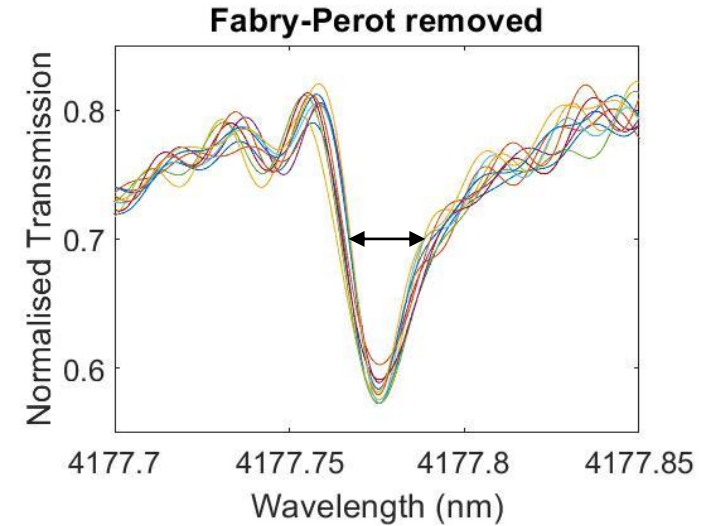


First High-Q Ring on SiGe in the MIR

- Resonance had Fano shape
- Fitting Fano function [1]:

$$\sigma(E) = D^2 \frac{(q + \Omega)^2}{1 + \Omega^2}$$

σ – spectrum
 $q = \cot(\delta)$ Fano parameter
 δ – phase shift between coupled states
 $D = 4\sin^2(\delta)$
 $\Omega = 2(E-E_0)/\Gamma$
 Γ – resonance width
 E_0 – resonance energy



[1] M.F. Limonov et al, *Fano resonances in photonics*, Nature photonics vol. 11, pp. 543-554, 2017

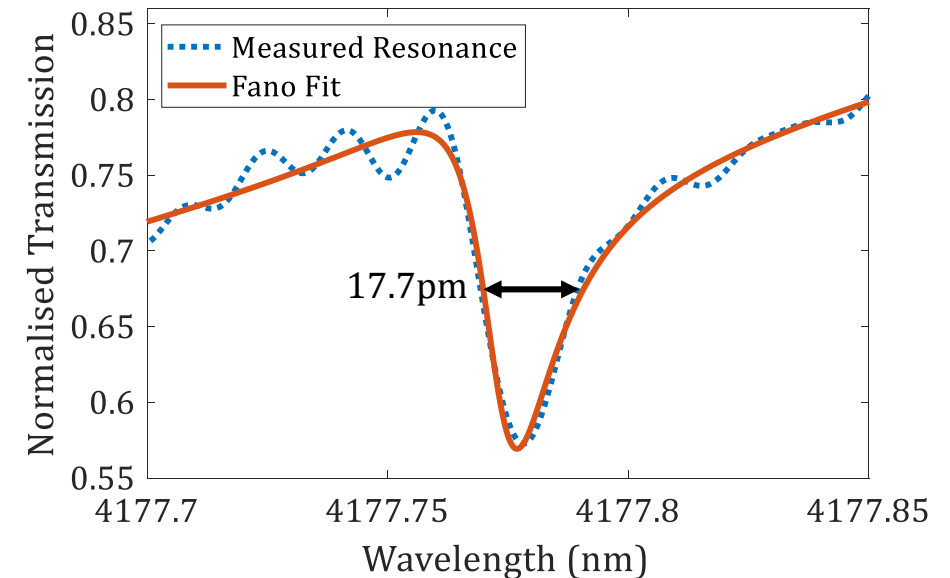
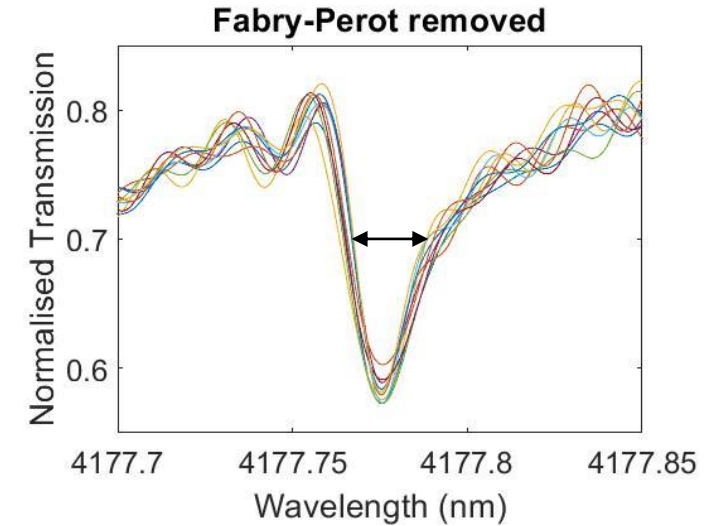
First High-Q Ring on SiGe in the MIR

- Resonance had Fano shape
- Fitting Fano function [1]:

$$\sigma(E) = D^2 \frac{(q + \Omega)^2}{1 + \Omega^2}$$

σ – spectrum
 $q = \cot(\delta)$ Fano parameter
 δ – phase shift between coupled states
 $D = 4\sin^2(\delta)$
 $\Omega = 2(E-E_0)/\Gamma$
 Γ – resonance width
 E_0 – resonance energy

- $\Gamma = 17.7 \text{ pm}$ ($Q_{\text{tot}} = 236,000$)



[1] M.F. Limonov et al, *Fano resonances in photonics*, Nature photonics vol. 11, pp. 543-554, 2017

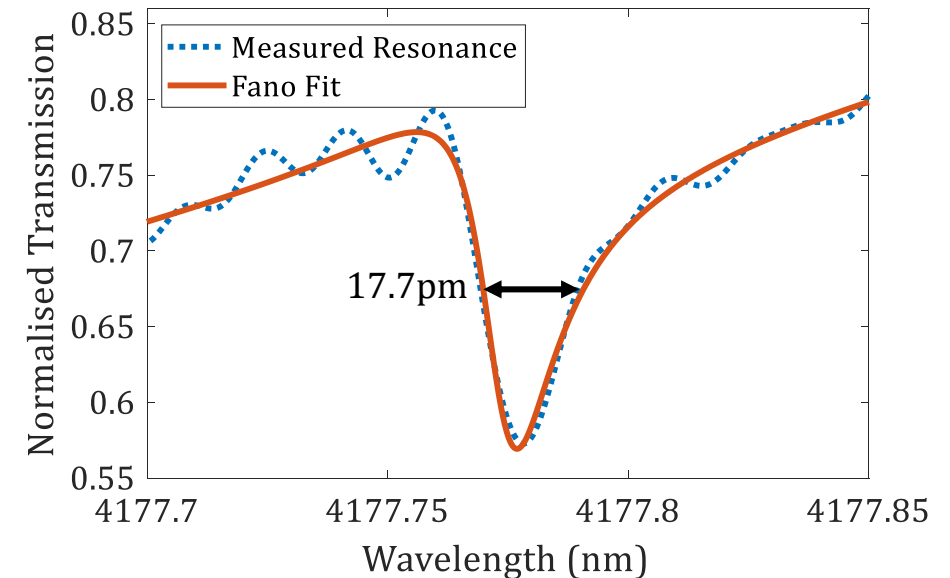
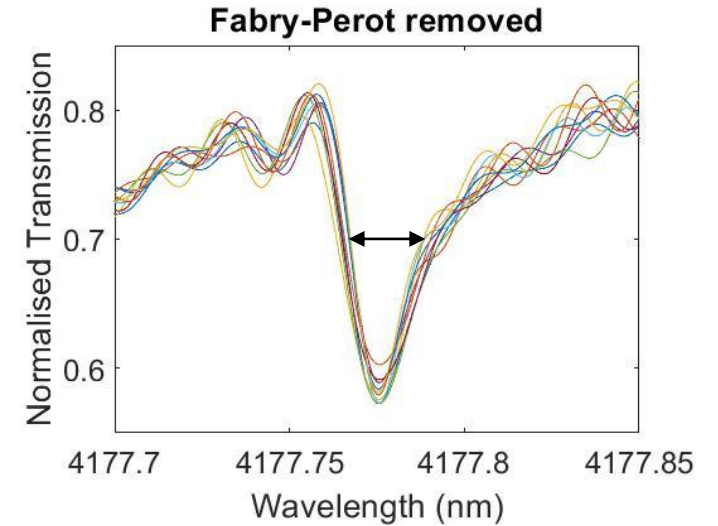
First High-Q Ring on SiGe in the MIR

- Resonance had Fano shape
- Fitting Fano function [1]:

$$\sigma(E) = D^2 \frac{(q + \Omega)^2}{1 + \Omega^2}$$

σ – spectrum
 $q = \cot(\delta)$ Fano parameter
 δ – phase shift between coupled states
 $D = 4\sin^2(\delta)$
 $\Omega = 2(E-E_0)/\Gamma$
 Γ – resonance width
 E_0 – resonance energy

- $\Gamma = 17.7$ pm ($Q_{\text{tot}} = 236,000$)
- Nature of Fano resonance not entirely clear



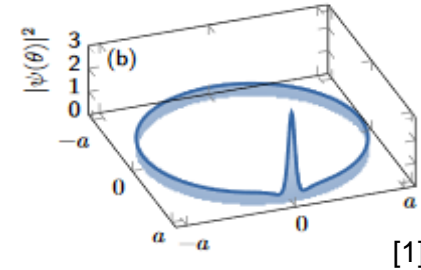
[1] M.F. Limonov et al, *Fano resonances in photonics*, Nature photonics vol. 11, pp. 543-554, 2017

Using our Experimental Q-factor Results for the Rings

Lugiato-Lefever equation

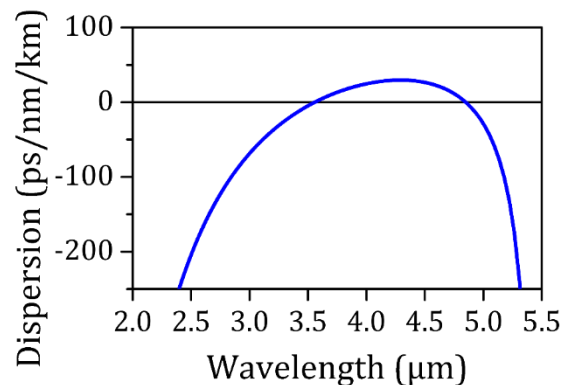
$$\frac{d\psi}{dt} = -(1 + i\alpha)\psi + i|\psi|^2\psi - i\frac{\beta}{2}\frac{\partial^2\psi}{\partial\theta^2} + F$$

ψ – Intracavity field
 F – External pump field intensity
 θ – azimuthal angle along circumference
 α – frequency detuning
 β – dispersion parameter
 (Loss is included in α and β)



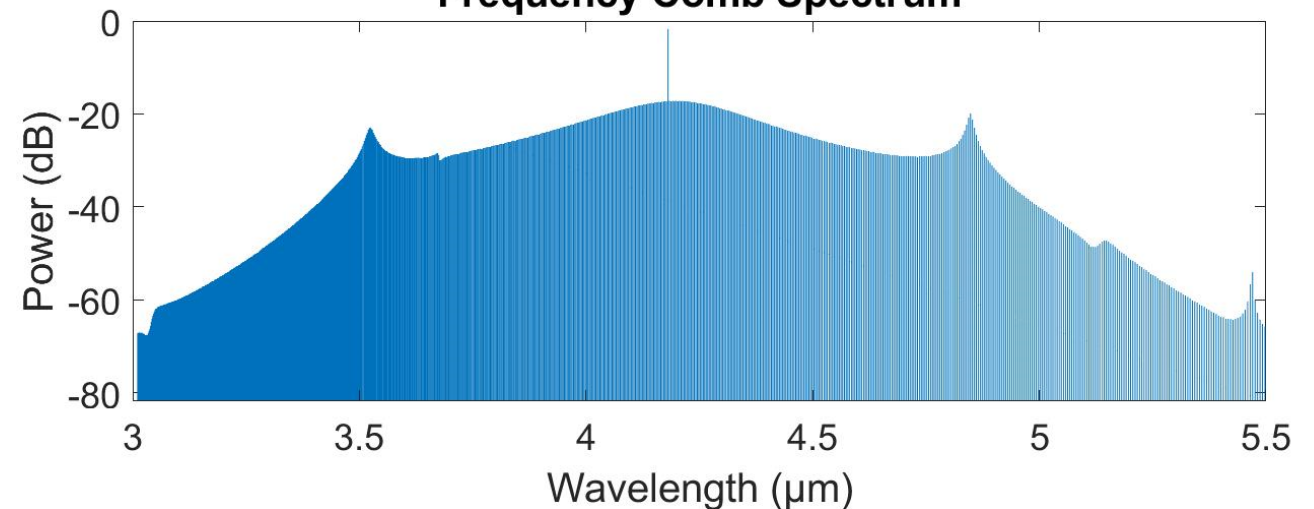
Simulation taking into account ring parameters:

- $R = 250 \mu\text{m}$
- $Q = 236,000$
- Waveguide nonlinear parameter $\gamma = 0.63 \text{ W}^{-1}\text{m}^{-1}$
- Threshold pump power $P_{\text{th}} = 200 \text{ mW}$
- Waveguide dispersion (simulated):



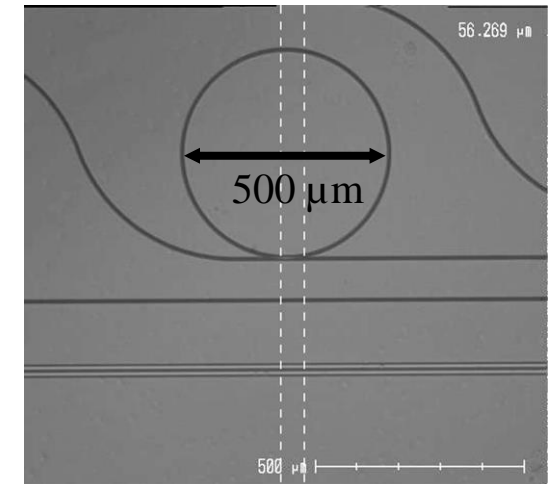
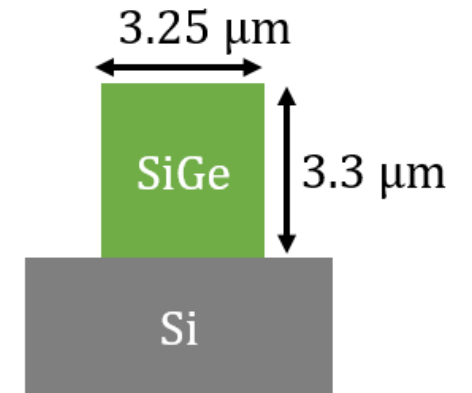
Soliton state at $P = 1.5 P_{\text{th}}$:

Frequency Comb Spectrum

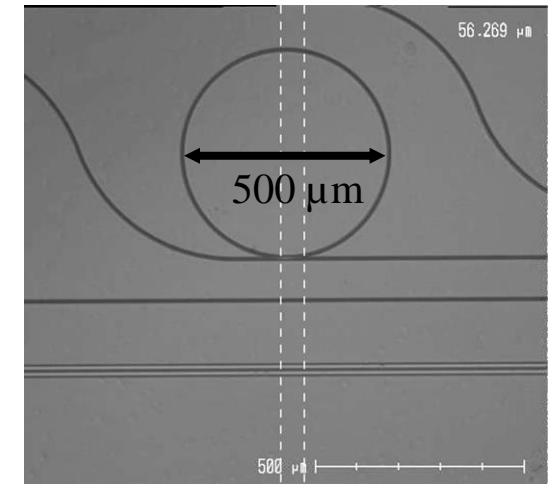
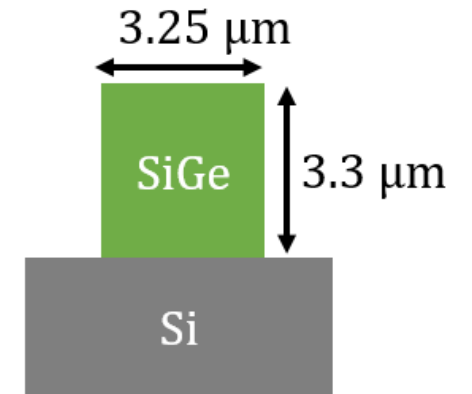


[1] C. Godey et al., Phys. Rev. A 86, 063814 (2014)

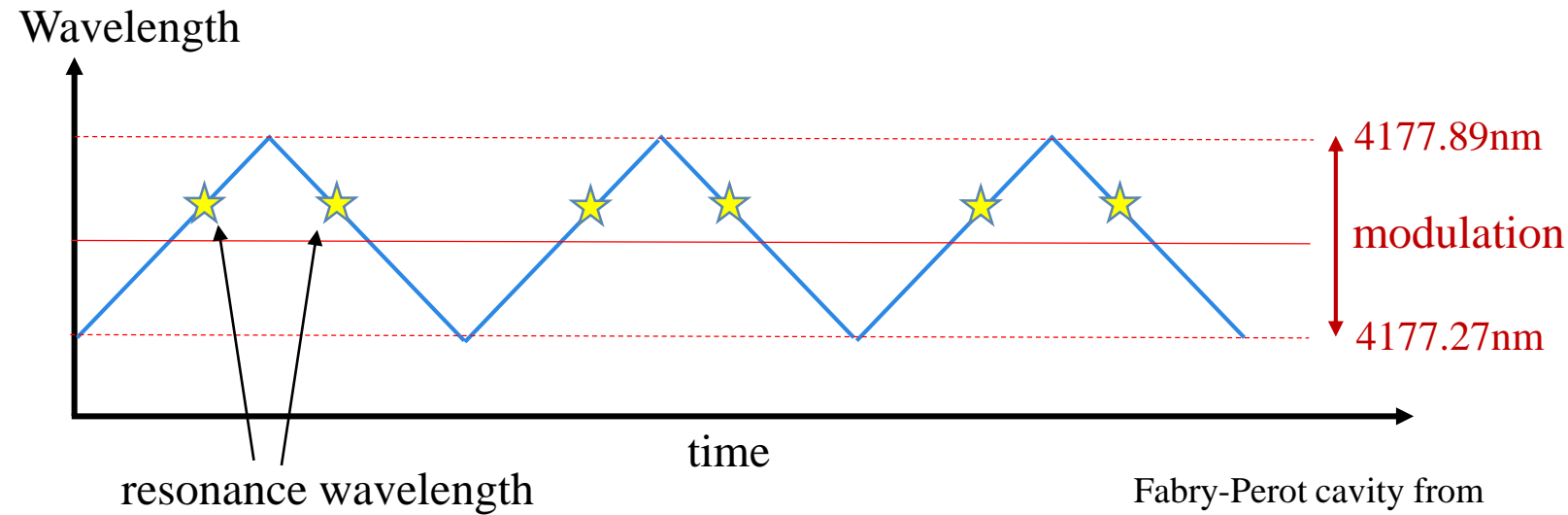
- First demonstration of an integrated high-Q ring resonator on SiGe in the MIR
- Loaded $Q_{\text{tot}} = 236,000$ at $\lambda = 4.18\mu\text{m}$ (intrinsic Q higher)
- Next batch will start fabrication soon (improved designs)
- Rings show great potential to be used for Kerr frequency comb generation very soon (now already promising for linear sensing applications)



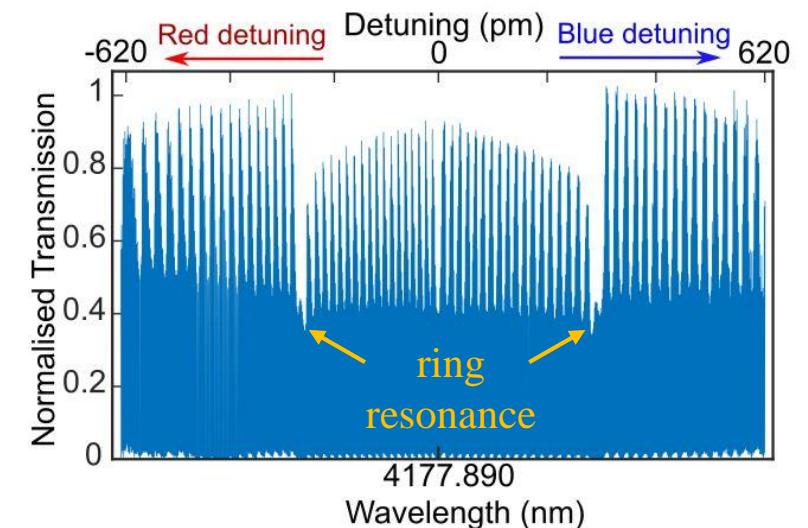
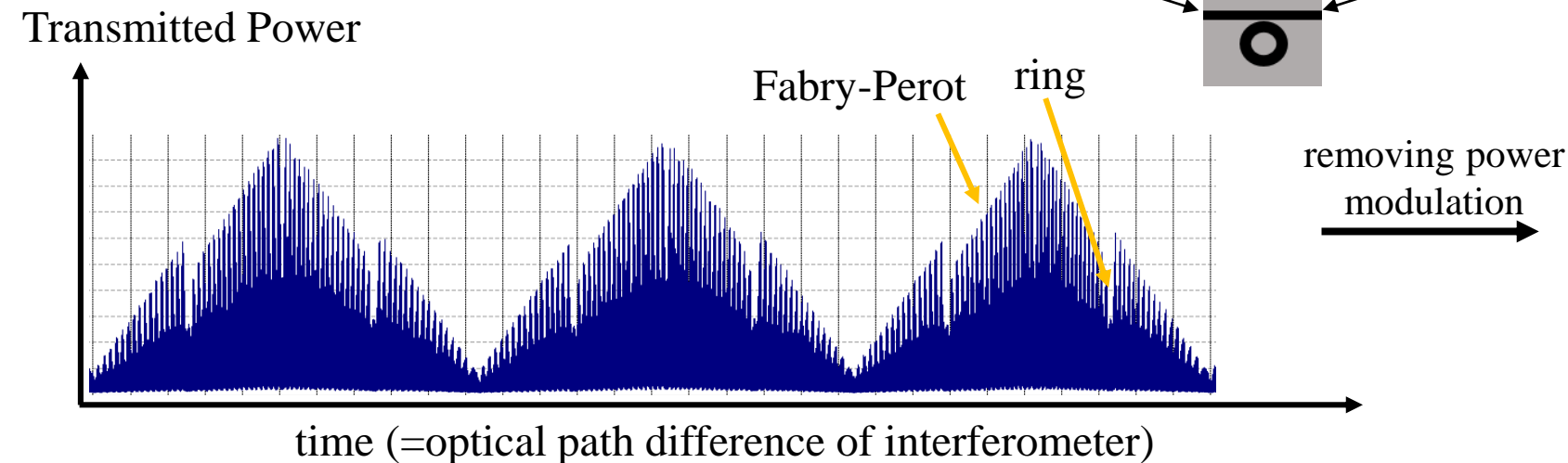
- First demonstration of an integrated high-Q ring resonator on SiGe in the MIR
- Loaded $Q_{\text{tot}} = 236,000$ at $\lambda = 4.18\mu\text{m}$ (intrinsic Q higher)
- Next batch will start fabrication soon (improved designs)
- Rings show great potential to be used for Kerr frequency comb generation very soon (now already promising for linear sensing applications)



Thank you for your attention! Questions?

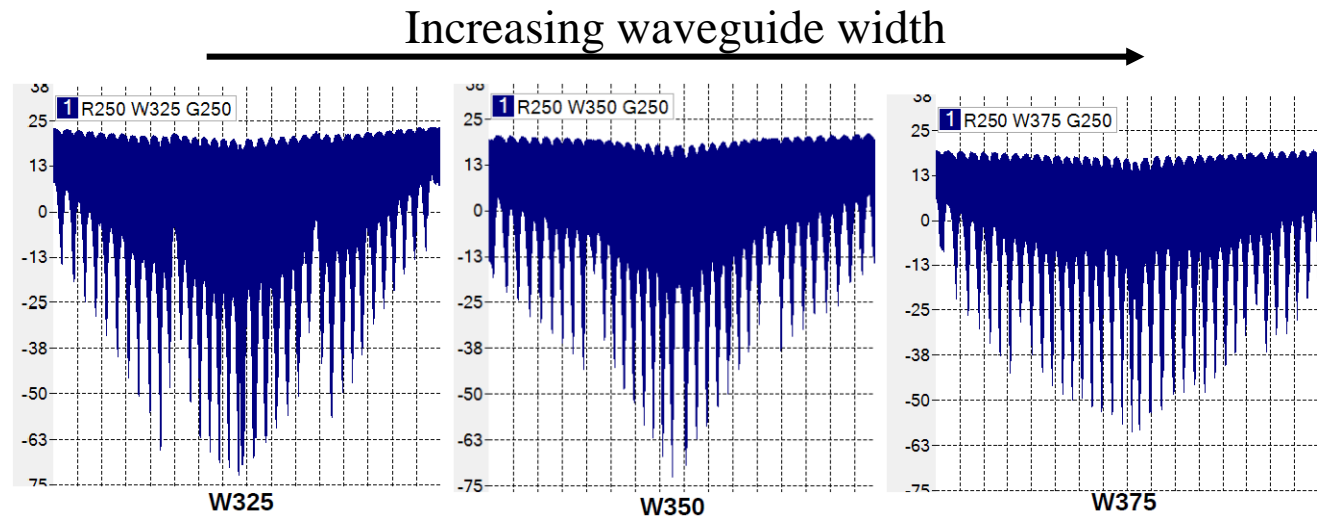


- Spectrum shows ring resonance and Fabry-Perot resonances from chip facets
- Ring resonance can be isolated

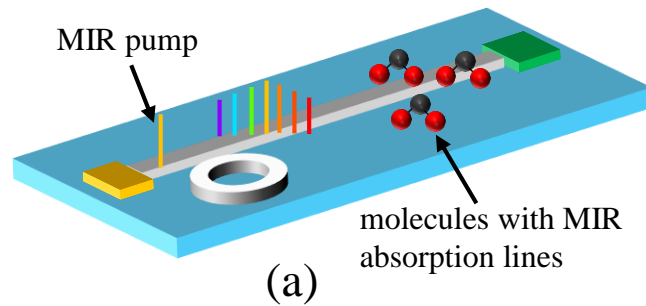


Investigation of Other Parameters

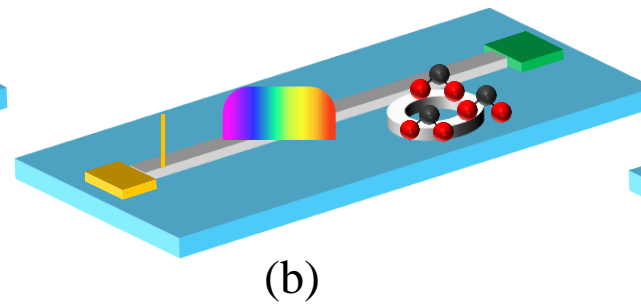
- Investigation of different radii, gaps, widths:
 - Q is decreasing if R goes below $250\mu\text{m}$ due to increased bending loss
 - Critical coupling likely not reached yet (no resonance observed for gap $> 250\text{nm}$)
 - Resonance depth weakens for increasing $w=3.25, 3.50, 3.75\mu\text{m}$



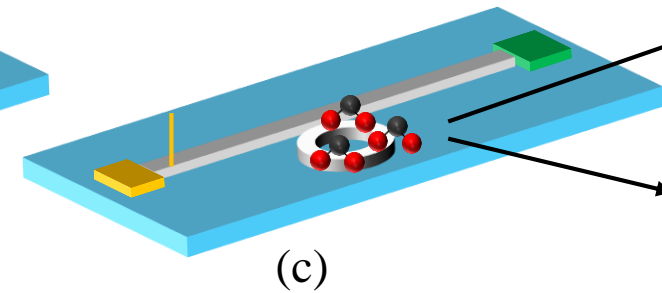
Many Different Sensing Schemes



Rings for Kerr frequency combs generation
(broadband light source for sensing)

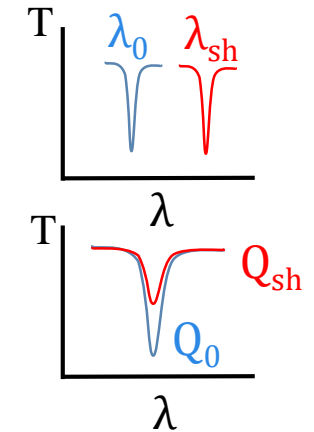


Rings for enhancement of light-molecule interaction
(for example with a supercontinuum source)



Rings as sensors through

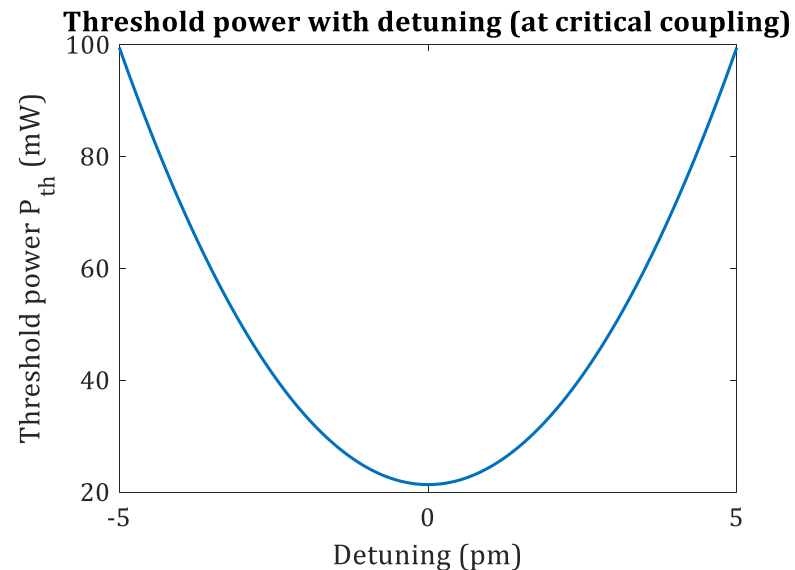
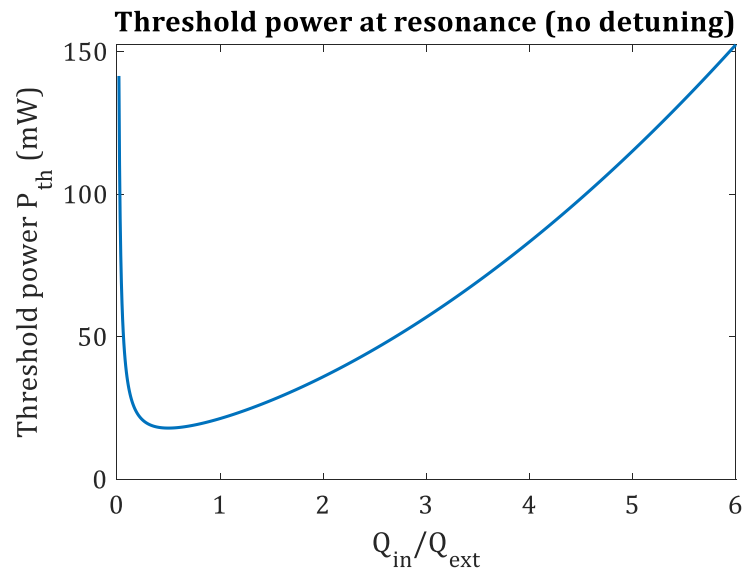
- Shift in resonance wavelength
- Shift of Q-factor



Calculated for our scenario

$$P_{th}(resonance) = \frac{\pi n_g^2 LA_{eff}}{4\lambda n_2 Q_{in}^2} \frac{(1 + K)^3}{K}$$

$$P_{th} = P_{th}(resonance) + \frac{n_g^2 LA_{eff} (\omega - \omega_0)^2}{2n_2 \omega c} \left(1 + \frac{1}{K}\right) \quad [1]$$



Used parameters:

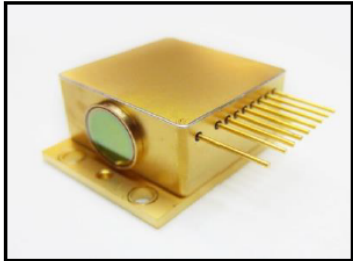
- Wavelength $\lambda = 4.18 \mu\text{m}$
- Ring radius $R = 250 \mu\text{m}$
- $Q = 236,000$
- $Q_{in} = 1,600,000$
- Group index $n_g = 3.67$
- Mode area $A_{eff} = 6.87 \mu\text{m}^2$
- $n_2 = 4 \times 10^{-14} \frac{\text{cm}^2}{\text{W}}$ (Optica paper)

[1] P.-S.Wang et al., *Sci Rep* 11.1 (2021): 1-10.



4.18 μm DISTRIBUTED FEEDBACK (DFB) QCL

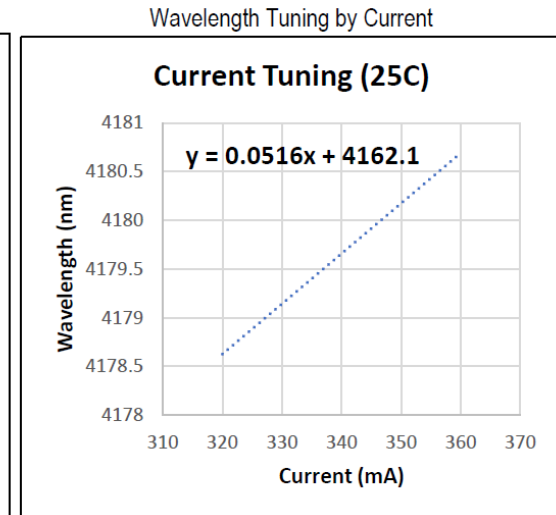
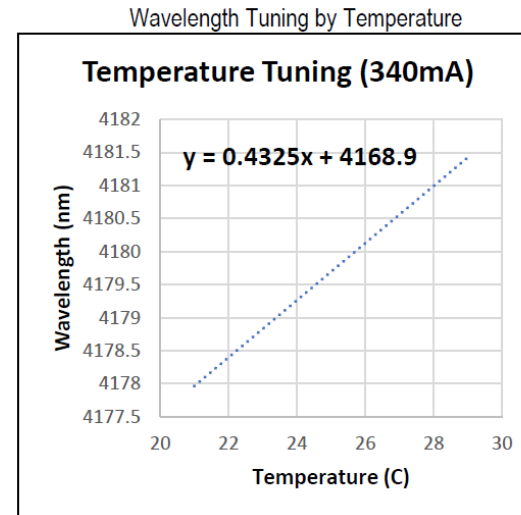
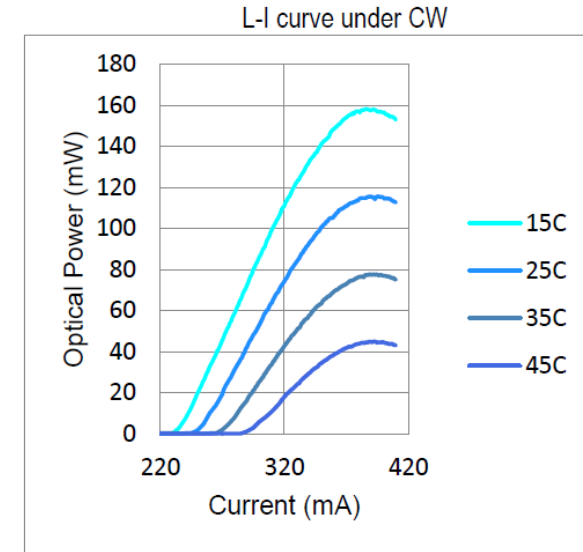
PART NO: HHL-19-64



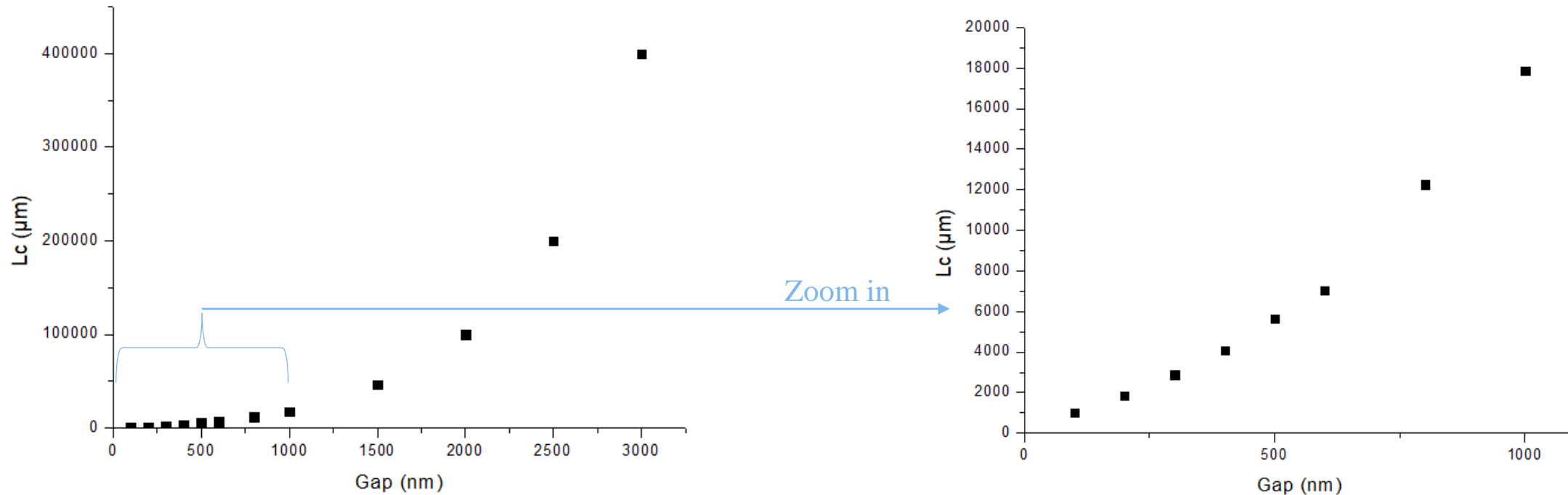
HIGH HEAT LOAD (HHL) PACKAGE

FEATURES

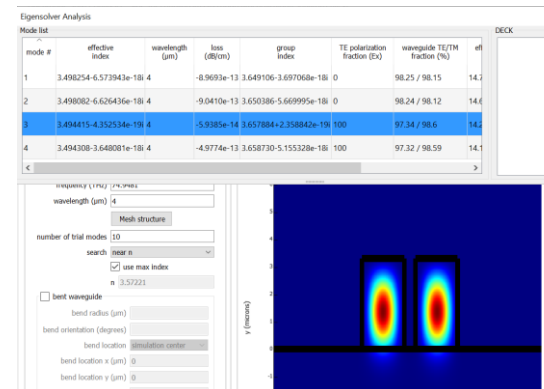
- Pulse or CW operated lasers
- Thermo-electrically cooled. External heat sink still required.
- Sensitive to electrostatic discharge, must have standard ESD precautions during handling
- Package dimensions (approx): 44.5 x 31.8 x 18.4 mm (excluding pins)



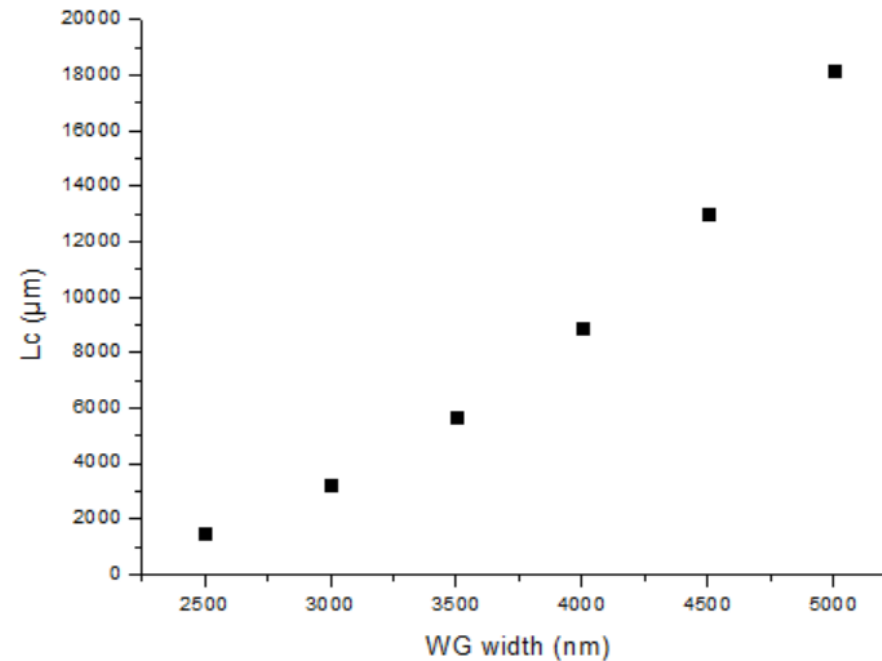
Dependence on Coupling Gap



- Example for the following parameters: $\lambda=4\mu\text{m}$, width= $3.5\mu\text{m}$, height $3.3\mu\text{m}$, SiGe-on-Si
- Calculation performed in Lumerical
- $L_C = \frac{\lambda_0}{2 \Delta n_{eff}}$ where Δn_{eff} is the difference between the two supermodes



Dependence on Waveguide Width



Example for the following parameters: $\lambda=4\mu\text{m}$, height= $3.3\mu\text{m}$, gap= 500nm , SiGe-on-Si
Calculation performed in Lumerical with the method from the previous slide

Conclusion: As expected intuitively, the coupling strength decreases with increasing waveguide width (the two mode centers are further apart and the evanescent field is weaker)

Some Examples of Coupling Lengths of SiGe and Ge resonators from Literature

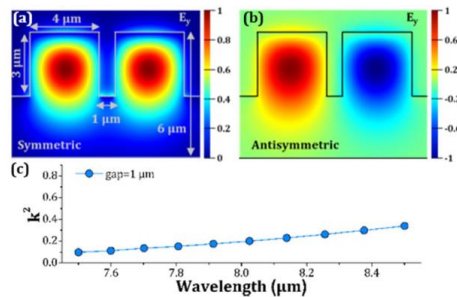
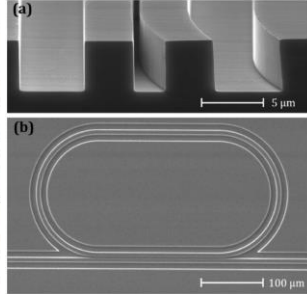


Broadband integrated racetrack ring resonators for long-wave infrared photonics

JOAN MANEL RAMIREZ,^{1,*} QIANKUN LIU,^{1,†} VLADYSLAV VAKARIN,^{1,†} XAVIER LE ROUX,¹ JACOPO FRIGERIO,² ANDREA BALLABIO,² CARLOS ALONSO-RAMOS,¹ ENRICO TALAMAS SIMOLA,² LAURENT VIVIEN,¹ GIOVANNI ISELLA,² AND DELPHINE MARRIS-MORINI¹

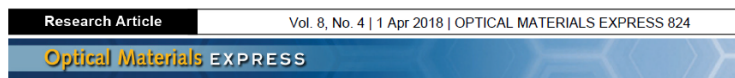
¹Centre de Nanosciences et de Nanotechnologies (C2N), Université Paris Sud, CNRS, Université Paris Saclay, 91405 Orsay, France
²L-NESS, Dipartimento di Fisica, Politecnico di Milano, Polo di Como, Via Anzani 42, 22100 Como, Italy
^{*}Corresponding author: joan.ramirez@c3-slab.fr

Long-wave infrared photonics is an exciting research field meant to revolutionize our daily life by means of key advances in several domains including communications, imaging systems, medical care, environmental monitoring, or multispectral chemical sensing, among others. For this purpose, integrated photonics is particularly promising owing to its compactness, mass fabrication, and energy-efficient characteristics. We present in this Letter, for the first time to the best of our knowledge, broadband integrated racetrack ring resonators operating within the crucial molecular fingerprint region. Devices show an operation bandwidth of $\Delta\lambda \approx 900$ nm with a central wavelength of $\lambda \approx 8$ μm , a quality factor of $Q \approx 3200$, and an extinction ratio of ER ≈ 10 dB around the critical coupling condition. These resonant structures establish the basis of a new generation of integrated building blocks for long-wave infrared photonics that opens the route towards miniaturized multi-target molecule detection systems. © 2019 Optical Society of America



$g = 1 \mu\text{m}$
 $L = 200 \mu\text{m}$
 Ge-rich SiGe

Simulation Lumerical: $L_c = 1800 \mu\text{m}$

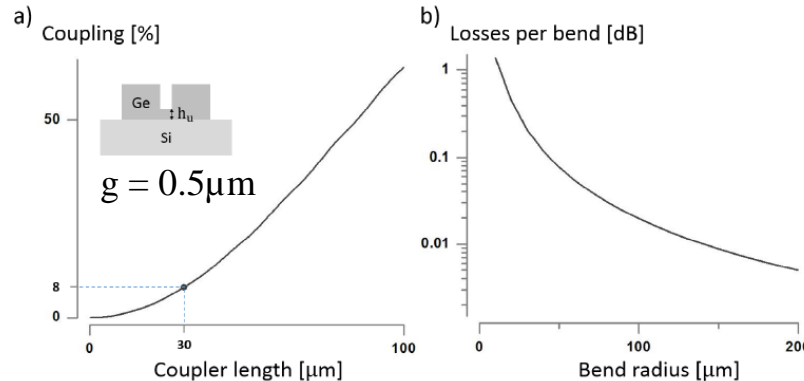


Mid-infrared Vernier racetrack resonator tunable filter implemented on a germanium on SOI waveguide platform [Invited]

SANJA RADOSAVLJEVIC,^{*} NURIA TEIGELL BENEITEZ, ANDREW KATUMBA, MUHAMMAD MUNEER, MICHAEL VANSLEMBROUCK, BART KUYKEN, AND GUNTHER ROELKENS

Photonics Research Group, Ghent University - imec, Technologiepark 15, 9052 Ghent, Belgium
 Center for Nano- and Biophotonics, Technologiepark 15, 9052 Ghent, Belgium
^{*}sanja.radosavljevic@ugent.be

Abstract: Currently, most widely tunable lasers rely on an external diffraction grating to tune the laser wavelength. In this paper we present the realization of a chip-scale Vernier tunable racetrack resonator filter on the Ge-on-SOI waveguide platform that allows for wide tuning (108 nm free spectral range) in the 5 μm wavelength range without any moving parts. The fabricated racetrack resonators have a loaded Q-factor of 20000, resulting in a side-peak suppression of more than 20 dB, which is more than sufficient for wavelength selection in an external cavity laser.



Simulation Lumerical: $L_c = 251 \mu\text{m}$

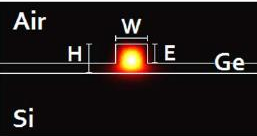


Germanium-on-silicon Vernier-effect photonic microcavities for the mid-infrared

BENEDETTO TROIA,¹ JORDI SOLER PENADES,² ALI Z. KHOKHAR,² MILOŠ NEDELJKOVIĆ,² CARLOS ALONSO-RAMOS,³ VITTORIO M. N. PASSARO,^{1,*} AND GORAN Z. MASHANOVICH²

¹Department of Electrical and Information Engineering, Politecnico di Bari, Via E. Orabona 4, 70125 Bari, Italy
²Optoelectronics Research Centre, University of Southampton, Southampton SO17 1BJ, UK
³Institut d'Electronique Fondamentale, Université Paris-Sud CNRS UMR 8622, Université Paris-Saclay F-91405 Orsay, France
^{*}Corresponding author: vittorio.passaro@poliba.it

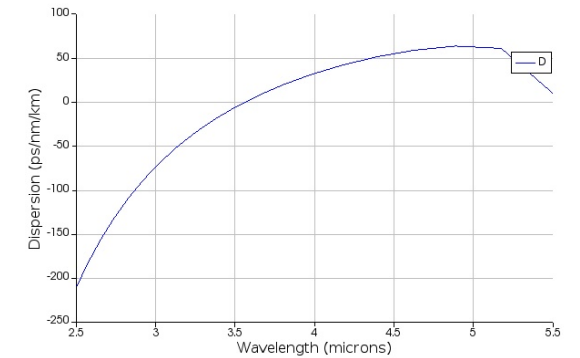
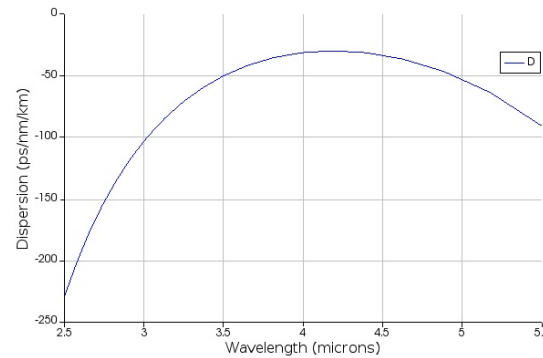
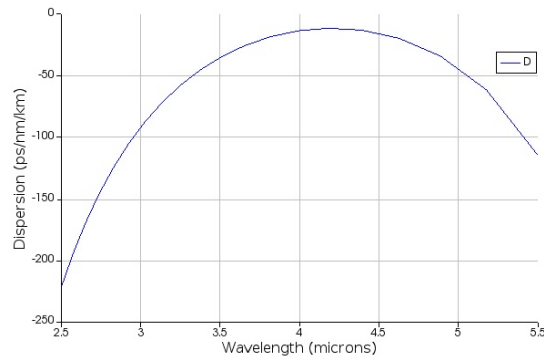
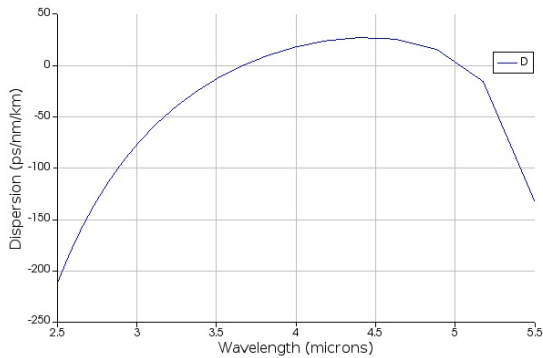
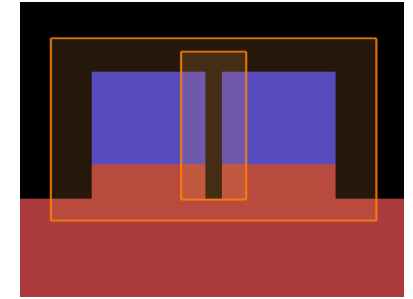
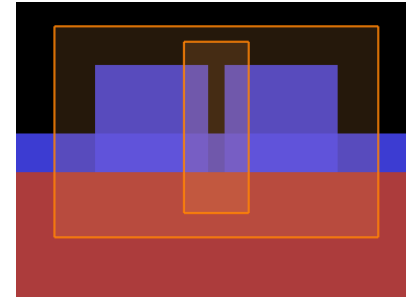
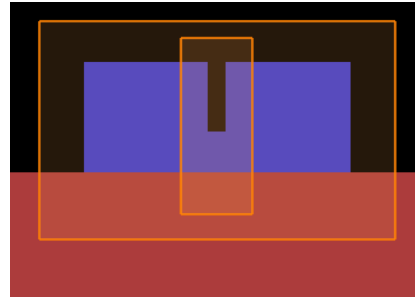
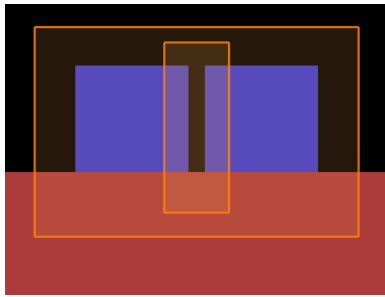
We present Vernier-effect photonic microcavities based on a germanium-on-silicon technology platform, operating around the mid-infrared wavelength of 3.8 μm . Cascaded racetrack resonators have been designed to operate in the second regime of the Vernier effect, and typical Vernier comb-like spectra have been successfully demonstrated with insertion losses of ~ 5 dB, maximum extinction ratios of ~ 23 dB, and loaded quality factors higher than 5000. Furthermore, an add-drop racetrack resonator designed for a Vernier device has been characterized, exhibiting average insertion losses of 1 dB, extinction ratios of up to 18 dB, and a quality factor of ~ 1700 . © 2016 Optical Society of America



Parameters	Vernier #A		Vernier #B	
	RR #A1	RR #A2	RR #B1	RR #B2
L (μm)	439.60	449.60	1039.30	1079.10
R (μm)	59	59	142	149
L_i (μm)	34.44	39.44	73.54	71.45
g_0 (nm)	450	450	650	650

Simulation Lumerical: $L_{c,TE} = 562 \mu\text{m}$, $L_{c,TM} = 520 \mu\text{m}$

Conclusion: The typical coupling lengths in literature for comparable platforms are lower than ours. But this likely comes from some differences, like gap underetching. So this is something we can also try if we want to increase the coupling

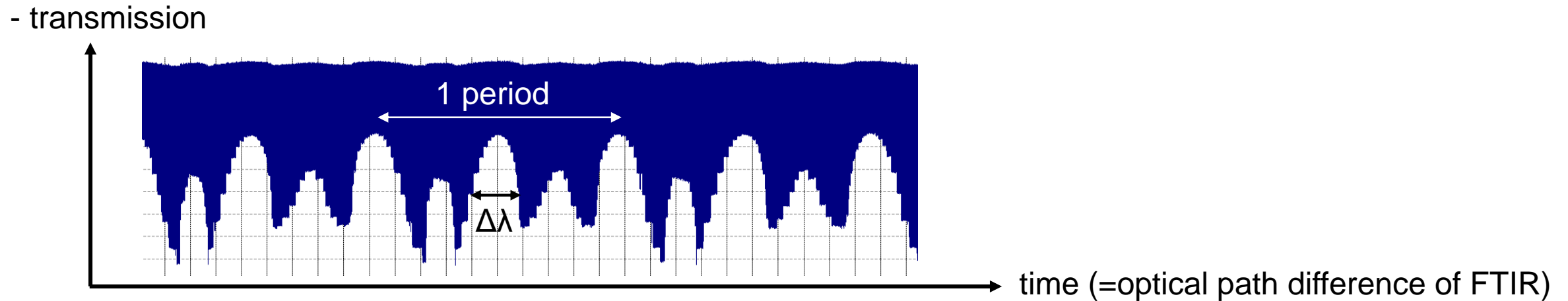


Example for the following parameters: width=3.5 μ m, gap=500nm, SiGe-on-Si

Calculation performed in Lumerical

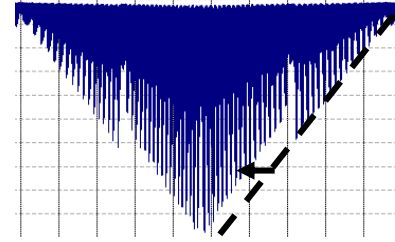
Conclusion: Underetching will move us to all-normal dispersion at some point. Overetching has the opposite effect, the anomalous dispersion gets stronger.

And hence narrowing down the resonance wavelength



- We know how much one period in time is in terms of wavelength, so we also know the width of the resonances
- We are sure that these are resonances from the chip, because if we heat the chip the resonances move
- $Q = 90\,000$ for this ring

To try to understand the jump in our ring resonator measurements



APPLIED PHYSICS LETTERS

VOLUME 80, NUMBER 6

11 FEBRUARY 2002

Sharp asymmetric line shapes in side-coupled waveguide-cavity systems

Shanhui Fan^{a)}

Department of Electrical Engineering, Stanford University, Stanford, California 94305

(Received 1 October 2001; accepted for publication 29 November 2001)

We show that, for an optical microcavity side coupled with a waveguide, sharp, and asymmetric line shapes can be created in the response function by placing two partially reflecting elements into the waveguides. In such a system, the transmission coefficient varies from 0% to 100% in a frequency range narrower than the full width of the resonance itself. We numerically demonstrate this effect by simulating the propagation of electromagnetic waves in a photonic crystal. © 2002 American Institute of Physics. [DOI: 10.1063/1.1448174]

$$t_s = \frac{(r^2 - 1)e^{2i\delta}(\omega - \omega_0)}{-e^{4i\delta}r^2(\omega - \omega_0 - i\gamma) - 2e^{2i\delta}(i\gamma)r + \omega - \omega_0 + i\gamma}$$

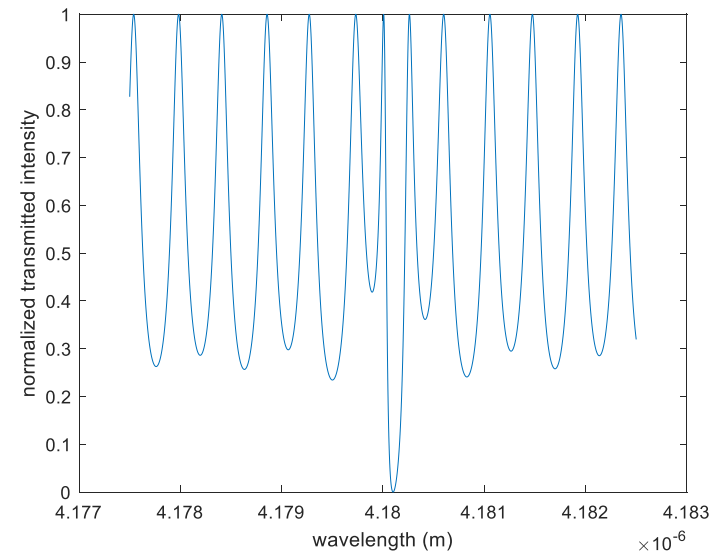
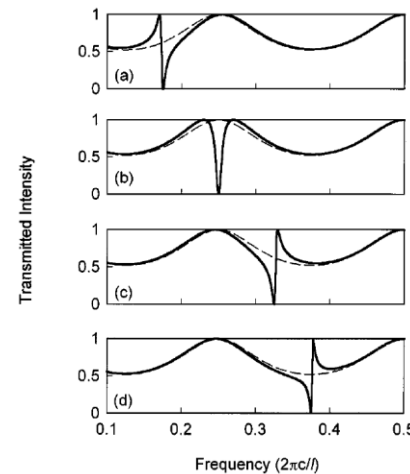
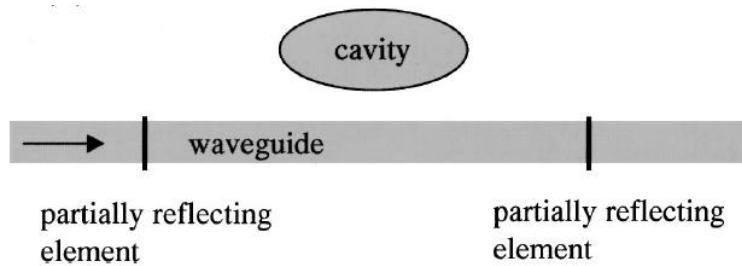
t_s – amplitude transmissivity

r – amplitude reflectivity at waveguide facet

δ – $\omega l/c$ phase shift aquired by waveguide mode (l – half length of Fabry-Perot cavity)

ω_0 – resonance frequency

γ – width of resonance



- “The shapes of the resonant features depend critically on the relative positions of the resonant frequency in relation to the background.”
- But no parameter combination seems to lead to a jump
- Can maybe still be useful to estimate resonance visibility

More general, not in the limit of a narrow ring resonance

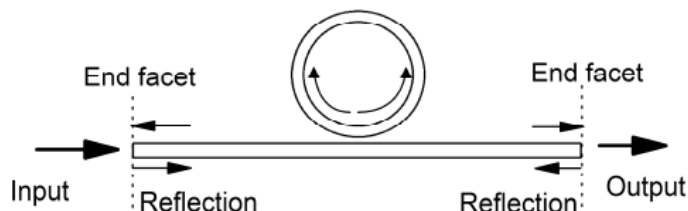
Highly sensitive silicon microring sensor with sharp asymmetrical resonance

Huaxiang Yi,¹ D. S. Citrin,²
and Zhiping Zhou^{1,2,*}

¹State Key Laboratory on Advanced Optical Communication Systems and Networks, Peking University, Beijing, 100871, China

²School of Electrical and Computer Engineering, Georgia Institute of Technology, Atlanta, 30318, USA and UMI 2958 Georgia Tech-CNRS, Georgia Tech Lorraine, 2-3 Rue Marconi, 57070 Metz, France
*zjzhou@pku.edu.cn

#120508 - \$15.00 USD Received 30 Nov 2009; revised 7 Jan 2010; accepted 21 Jan 2010; published 27 Jan 2010
(C) 2010 OSA 1 February 2010 / Vol. 18, No. 3 / OPTICS EXPRESS 2967



$$T = T_{FP} \begin{bmatrix} e^{i\varphi} & 0 \\ 0 & e^{-i\varphi} \end{bmatrix} T_r \begin{bmatrix} e^{i\varphi} & 0 \\ 0 & e^{-i\varphi} \end{bmatrix} T_{FP},$$

$$T_r = \begin{bmatrix} 1 - \frac{iW}{\omega - \omega_0} & \frac{-iW}{\omega - \omega_0} \\ \frac{iW}{\omega - \omega_0} & 1 + \frac{iW}{\omega - \omega_0} \end{bmatrix},$$

$$T_{FP} = \frac{1}{i\sqrt{1-r^2}} \begin{bmatrix} -1 & -r \\ r & 1 \end{bmatrix}$$

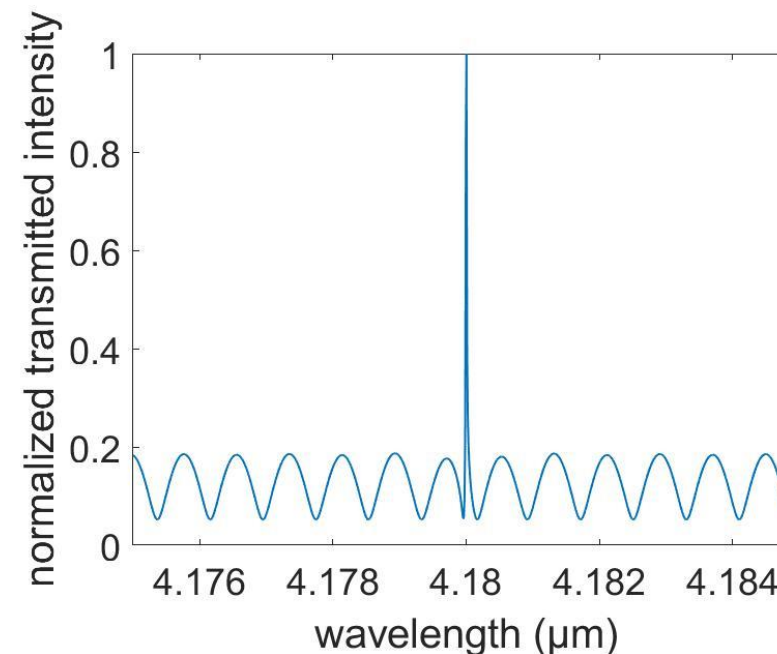
T – transfer matrix

r – amplitude reflectivity at waveguide facet

$\varphi = \omega l/2c$ phase shift acquired by waveguide mode (l – length of Fabry-Perot cavity)

ω_0 – resonance frequency

W – width of resonance (HWHM)



Does not reproduce the asymmetry either

Through supercontinuum generation



Mid-infrared octave spanning supercontinuum generation to 8.5 μm in silicon-germanium waveguides

MILAN SINOBAD,^{1,2,7} CHRISTELLE MONAT,¹ BARRY LUTHER-DAVIES,³ PAN MA,³ STEPHEN MADDEN,³ DAVID J. MOSS,⁴ ARNAN MITCHELL,² DAVID ALLIOUX,¹ REGIS OROBTCHOUK,¹ SALIM BOUTAMI,⁵ JEAN-MICHEL HARTMANN,⁵ JEAN-MARC FEDELI,⁵ AND CHRISTIAN GRILLET^{1,6}

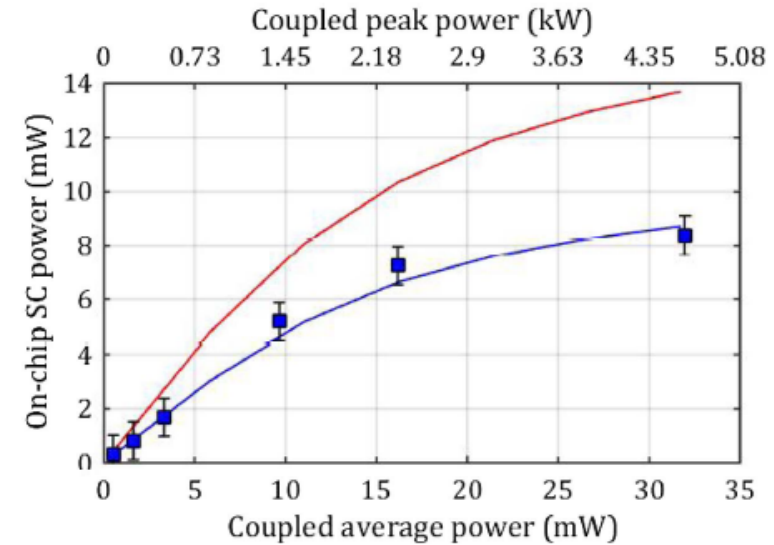
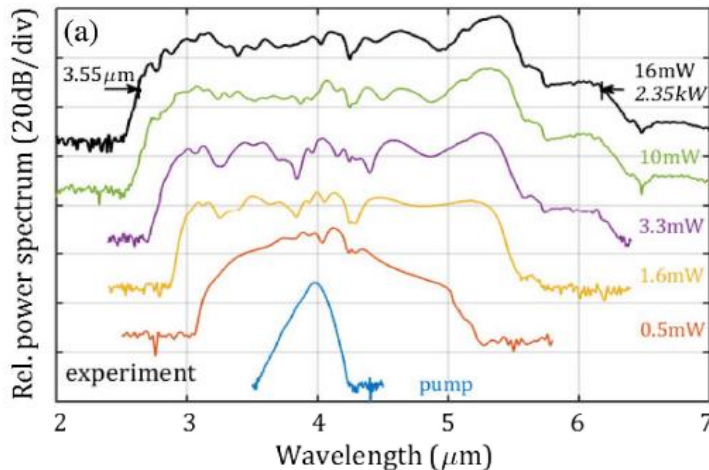
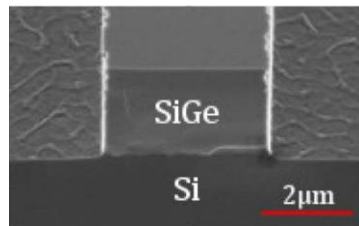


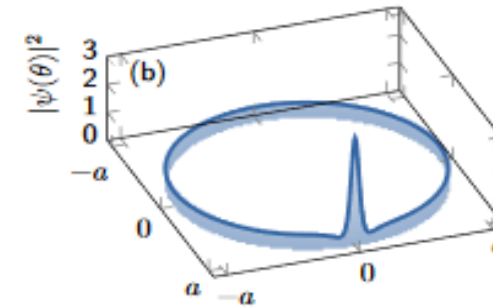
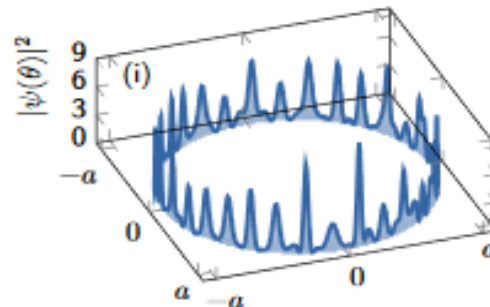
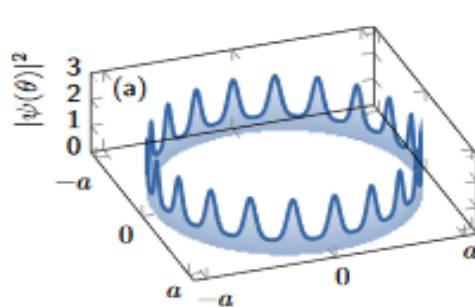
Fig. 5. On-chip SC power versus coupled average power measured for the 7 cm long waveguide (1) in TE at 4.0 μm (blue squares), simulated results for the 7 cm waveguide (blue line) and simulated results for a 2 cm long similar waveguide (red line).

Fit gives $\gamma = 0.63 \text{ W}^{-1}\text{m}^{-1}$

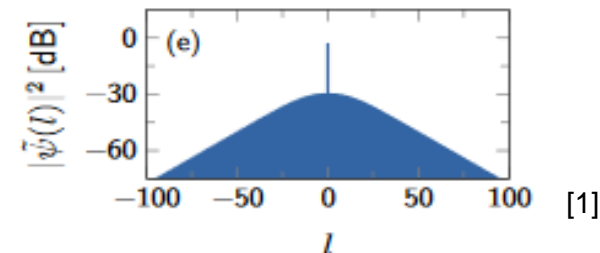
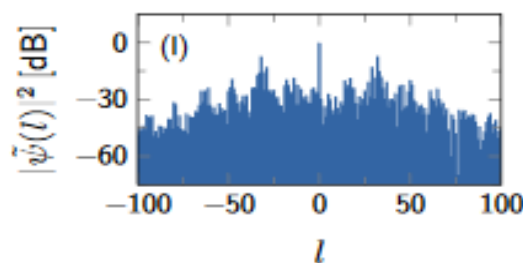
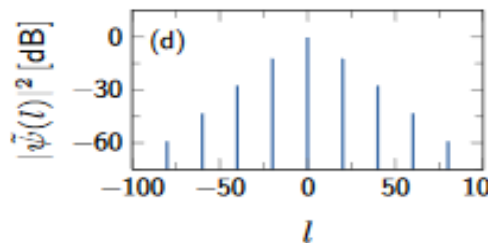
Lugiato-Lefever equation

$$\frac{d\psi}{dt} = -(1 + i\alpha)\psi + i|\psi|^2\psi - i\frac{\beta}{2}\frac{\partial^2\psi}{\partial\theta^2} + F$$

Cavity field



Spectrum



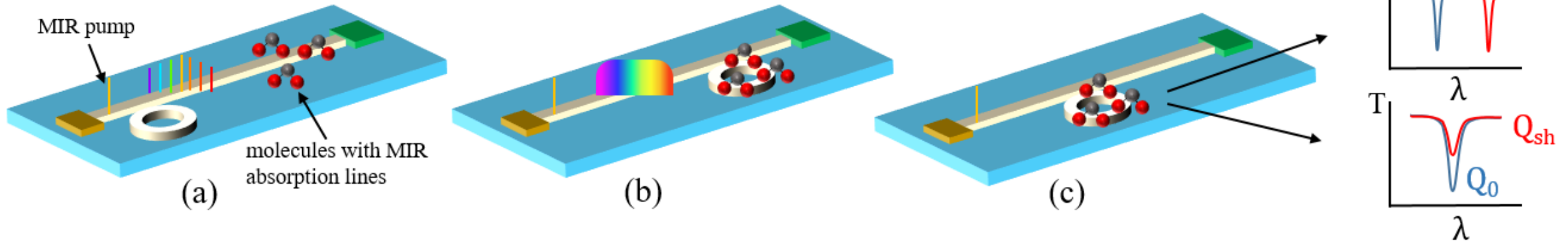
Turing rolls

Chaos

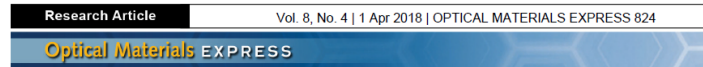
Soliton

[1] C. Godey et al., Phys. Rev. A 86, 063814 (2014)

Sensing schemes:



Rings for filters:



Mid-infrared Vernier racetrack resonator tunable filter implemented on a germanium on SOI waveguide platform [Invited]

SANJA RADOSAVLJEVIC,* NURIA TEIGELL BENEITEZ, ANDREW KATUMBA, MUHAMMAD MUNEEB, MICHAEL VANSLEMBROUCK, BART KUYKEN, AND GUNTHER ROELKENS

Photonics Research Group, Ghent University - imec, Technologiepark 15, 9052 Ghent, Belgium
 Center for Nano- and Biophotonics, Technologiepark 15, 9052 Ghent, Belgium
 *sanja.radosavljevic@ugent.be

